Electron transfer through a molecular wire: Consideration of electron-vibrational coupling within the Liouville space pathway technique

V. May
Institüt für Physik, Humboldt-Universität zu Berlin, Hausvogteiplatz, D-10117 Berlin, Federal Republic of Germany
(Received 15 January 2002; revised manuscript received 16 August 2002)

To fully account for electron-vibrational coupling and vibrational relaxation in the course of electron motion through a molecular wire a density operator approach is utilized. If combined with a particular projection operator technique a generalized master equation can be derived which governs the populations of the electronic wire states. The respective memory kernels are determined beyond any perturbation theory with respect to the electron-vibrational coupling and can be classified via so-called Liouville space pathways. An ordering of the different contributions to the current-voltage characteristics becomes possible by introducing an electron transmission coefficient which describes ballistic as well as inelastic electron transport through the wire. The general derivations are illustrated by numerical calculations which demonstrate the drastic influence of the electron-vibrational coupling on the wire transmission coefficient as well as on the current-voltage characteristics.

DOI: 10.1103/PhysRevB.66.2454XX PACS number(s): 85.65.+h, 73.61.Ph, 34.10.+x, 34.30.+h

I. INTRODUCTION

It is an old dream of molecular electronics to handle single molecules as active elements of nanoscale electric circuits.[1–4] Meanwhile, is became possible to attache microelectrodes to single molecules and to study their conductivity as well as to derive related *IV* characteristics (see, for example, Refs. 5–7, and the recent overview in Ref. 8). This experimental progress initiated a number of theoretical studies aimed at reproducing measured *IV* characteristics (compare Refs. 9–13, and references therein as well as the review papers of Refs. 14 and 15).

Such studies concern an accurate classification and computation of all molecular wire levels involved in the electron transfer. Furthermore it is of great interest to understand in which manner the coupling of the wire to the electrodes modifies the wire states. This may concern short-range couplings defined by the concrete type of chemical bond (see, e.g., Refs. 12 and 16). But also long-range Coulomb effects can come into play, which in the most simple case are accounted for via so-called mirror charge effects.[17,18] The presence of the applied voltage may change the molecular orbitals of the wire in a manner which should be determined self-consistently during the computation of the orbitals and which decides on the voltage drop over the wire.[19] But it also decides whether the electron transfer through the wire is a single-electron transfer or if two or more electrons are involved simultaneously.[10,18,20,21]

It is typical for all these approaches that the electron conduction of the wire is described as the result of a completely ballistic transport characterized by the transfer rate $k_{L\rightarrow R}$ from the left to the right electrode (see also Sec. III A). However, a number of recent computations aimed to include inelastic-scattering processes of the transferred electron at molecular vibrations.[22–28] The case of very slow vibrations where the electron-vibrational coupling can be handled as static disorder has been discussed in Ref. 22. In Ref. 24 electron-vibrational coupling was embedded into a generalization of the Landauer theory. An approach based on the Su-Schrieffer-Heeger model was used in Refs. 23, 25, and 27, whereas the Redfield theory could be applied in Ref. 26 (see also Ref. 15). A treatment which incorporates the coupling to a single vibrational mode in an exact way has been presented in Ref. 28. But it neglects electronic coherences which are of importance if one takes a description beyond a pure hopping transfer.

Of course such treatments are of interest whenever the coupling of the wire levels to the continuum of electrode states is weak enough. In the contrary case the broadening of the wire levels by the coupling to the electrode levels may dominate the transmission. This would be the case if chemisorption of the wire to the electrode atoms appears, for example, to be observed for paradithiohydroquinone on a gold electrode and is described in Ref. 6 (see also the computation in Ref. 13). If the wire is noncovalently attached to the electrode (as is the case for the DNA strands studied in Ref. 5) this continuum-induced broadening should be less dominant and inelastic effects of the electron transmission within the wire may have a noticeable influence. Or in other words, if the wire-level broadening due to the coupling to electrode levels becomes smaller than characteristic vibrational energies the latter may determine all the *IV* characteristics of the wire. It is just this case we will concentrate on in the following. (An approach which accounts for both effects, wire-level broadening and formation of vibrational substates, will be given elsewhere.[29]) In particular we will profit from the theory describing electron transfer through molecular donor–acceptor complexes

From standard electron transfer theory the importance of the proper description of electron-vibrational coupling is obvious (see the excellent overviews in Ref. 30). In the framework of this theory the mentioned ballistic transport is known as superexchange electron transfer. For the present example the superexchange mechanism dominates charge motion when the wire levels to be occupied by the transferred electron [the adiabatic lowest unoccupied molecular orbital (LUMO) levels] are far away from the electrode lev-

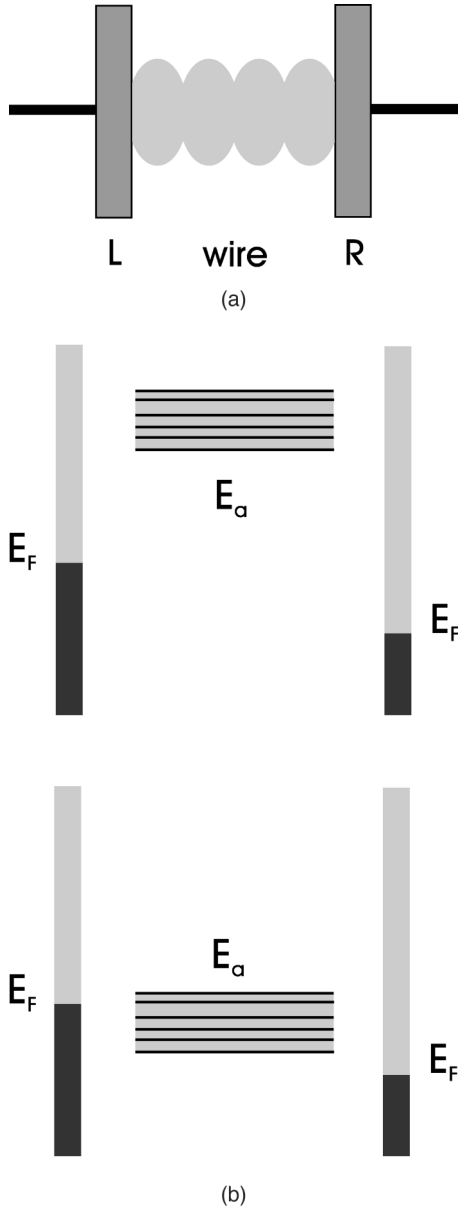

FIG. 1. (a) Scheme of a molecular wire embedded between a left (L) and right (R) microelectrode. (b) Energy-level scheme of the electrode–molecular-wire–electrode system of (a). The dark part of the left and right electrodes stands for the Fermi sea. The block in the middle gives the set of adiabatic states of the wire realized if the wire is populated by a single excess electron. Voltage bias is chosen to have a resulting electron motion from the left to the right. Upper part: Wire levels are far away from the Fermi energies (scheme of superexchange electron transfer). Lower part: Wire levels positioned in the region of the Fermi energies (scheme of hoppinglike electron transfer).

els (see the upper part of Fig. 1). In contrast, the transfer may proceed as a hoppinglike process (sequential electron transfer) if the wire levels are positioned near the energies of the electrode levels. If the applied voltage is increased one may change from one type of electron transfer to the other. Obviously, within a single *IV* characteristic both mechanisms may act and a comprehensive theory is required which accounts for both types of electron transfer mechanisms as well as the transition regime between them.

A unifying description of all electron transfer mechanisms is achieved when starting with a density-matrix theory formulated in the properly chosen electron-vibrational states (cf, e.g., Ref. 31). The complete set of density-matrix elements is of interest if, for example, optical experiments on so-called ultrafast electron transfer are considered. In the present case of *IV* characteristics, however, one only needs the net current of charge transfer through the wire, and it suffices to calculate the total electronic state populations. Such a description of electron transfer has been already given in Refs. 32 and 33 for two- and three-site systems. It directly leads to (generalized) rate equations for the electronic state population and simultaneously accounts, via respective rate expressions, for the superexchange and sequential mechanisms.

Here such a density-matrix treatment of electron transfer reactions will be adopted to account for inelastic contributions to the entire electron transport through molecular wires. This is done by including vibrational degrees of freedom (DOF), considering relaxation of the active vibrational coordinates (the reaction coordinates), and utilizing techniques of dissipative quantum dynamics.[31,34,35] As a result (generalized) rate equations for the electronic state population can be derived where the rate expressions are given as an expansion with respect to the electrode-wire interaction matrix elements, but incorporates electron-vibrational coupling in an exact way. The type of the expansion to be used can be classified by so-called Liouville space pathways.[33] According to the mentioned expansion the rates account for electronic and vibrational coherence, and in this manner they are well beyond simple hopping rates for electrode-wire transitions. In a certain limit the approach reproduces standard formulas for the electron transmission through a molecular wire (see, e.g., Ref. 15).

Since the present paper mainly focuses on the general scheme for the incorporation of electron-vibrational coupling into the studies of charge motion through molecular wires we use the simple model for the wire-electrode system as given in Fig. 1. We assume that the wire electronic states and all relevant types of vibrations are given quantities and that their dependence on the applied voltage as well as the voltage drop across the wire is known. Intrawire coupling may be assumed either to be strong or very weak. In the latter case every wire level can be described as a level being decoupled from the others. In the first case, i.e., when the wire internal relaxation should be fast compared to the electron motion a thermal equilibrium among the different levels can be provided.

The paper is organized as follows. In the next section the model together with the basic density-matrix treatment is given. The derivation of rate equations for the complete electronic state populations (of the two electrodes and the adiabatic wire states) and related electron transfer rates up to the fourth order with respect to the electrode-wire coupling are explained in Sec. III. Numerical illustrations can be found in Sec. VI. Based on a regular tight-binding model the wire states are introduced and the various contributions to the

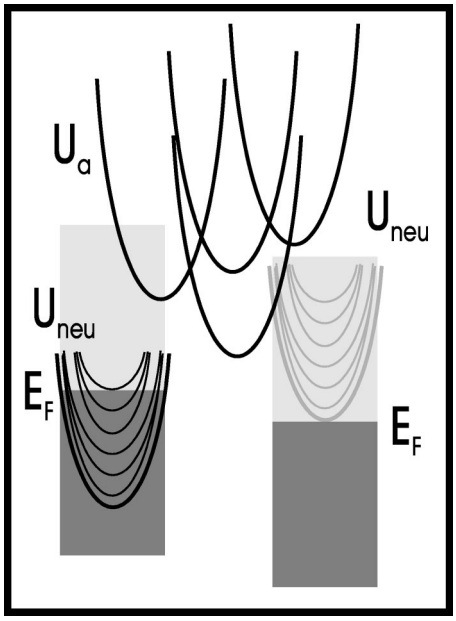

FIG. 2. Potential-energy surface scheme of the electrode-wire-electrode system of Fig. 1. For the left electrode only those potential-energy surfaces U_{neu} are shown which correspond to populated electron levels [below $E_F^{(L)}$]. In the case of the right electrode the U_{neu} are drawn referring to empty levels [above $E_F^{(R)}$]. The middle part contains the potential-energy surface U_a of the adiabatic wire states. (To be able to distinguish the different potential-energy surfaces from one another horizontal displacement has been strongly enlarged.)

transition rates of the fourth order with respect to the wire-electrode coupling are discussed. Finally, *IV* characteristics for a two-state wire are presented. The paper ends with some concluding remarks.

II. THE MODEL AND BASIC DENSITY OPERATOR EQUATIONS

According to the electrode-wire-electrode system introduced in Fig. 1 we separate the complete Hamiltonian into a wire part, the electrode contributions, and a respective coupling,

$$H = H_{\mathrm{wire}} + H_{\mathrm{el}} + H_{\text{el-wire}}. \tag{1}$$

For the Hamiltonian H_{wire} we provide an expansion with respect to adiabatic wire states φ_a which refer to LUMO levels occupied by the excess electrons (the certain limitations inherent to such a single-electron approach are discussed, for example, in Ref. 36):

$$H_{\mathrm{wire}} = \sum_a \ (\hbar\varepsilon_a + H_a)|\varphi_a\rangle\langle\varphi_a|. \tag{2}$$

$H_a = T_{\mathrm{neu}} + \Delta U_a$ denotes the vibrational Hamiltonian which belongs to the state φ_a (see Fig. 2). For notational convenience we split off the minimum $\min U_a = U_a^{(0)} \equiv \hbar\varepsilon_a$ of the complete potential-energy surface U_a. The remaining difference ΔU_a appears in the vibrational Hamiltonian.

The Hamiltonian which describes the vibrational dynamics of the neutral wire (if the excess electron is absent) is written as H_{neu}. It will be combined with the band energies $E_{X\mathbf{k}} \equiv \hbar\varepsilon_{X\mathbf{k}}$ $(X = L,R)$. Consequently, the electrode Hamiltonian reads

$$H_X = \sum_{\mathbf{k}} \ (\hbar\varepsilon_{X\mathbf{k}} + H_{\mathrm{neu}})|\varphi_{X\mathbf{k}}\rangle\langle\varphi_{X\mathbf{k}}|. \tag{3}$$

For further use we introduce states φ_m where m should comprise the wire electronic quantum numbers a as well as those of the two electrodes, i.e., $(X\mathbf{k})$.

All vibrational Hamiltonians introduced so far are defined with respect to the set $Q = \{Q_j\}$ of active vibrational coordinates (see the scheme in Fig. 2). At present there is no chance for an *ab initio* calculation of potential-energy surfaces U_a of the wire. Therefore, one has to make reasonable assumptions, from which the most basic provides surfaces for uncoupled harmonic vibrations where the equilibrium position has been shifted depending on the actual electronic state the excess electron occupies. (Possibly, the adiabatic levels may be connected by nonadiabatic couplings $\theta_{a,b}$.) The vibrational eigenstates will be denoted as χ_{mM} with the set M of vibrational quantum numbers. The respective vibrational energies read $\hbar\omega_{mM}$ [because of Eqs. (2) and (3) they start at the zero-point energy; for $m = X$ we drop the electronic index to get ω_M].

Finally we give the coupling Hamiltonian between the wire and the electrodes as

$$H_{\text{el-wire}} = \sum_{\mathbf{k},a} \ (V_{L\mathbf{k},a}|\varphi_{L\mathbf{k}}\rangle\langle\varphi_a| + V_{a,R\mathbf{k}}|\varphi_a\rangle\langle\varphi_{R\mathbf{k}}|) + \text{H. c.} \tag{4}$$

In a general treatment the applied voltage has to be accounted for self-consistently within the electronic structure calculation for the wire.

Likewise we can introduce a notation of the electrode-wire coupling which directly accounts for the continuous electronic energy levels of the electrodes. Therefore the electrode density of states

$$\mathcal{N}_X(\omega) = \sum_{\mathbf{k}} \ \delta(\omega - \varepsilon_{X\mathbf{k}}) \tag{5}$$

is introduced. This enables us to replace the wire-electrode coupling matrix elements of Eq. (4) by $V_{X,a}(\omega)$.

The models introduced so far will be completed by a coupling of the set Q of active vibrational coordinates to remaining passive coordinates.[31,30] These coordinates are denoted as $Z = \{Z_\xi\}$ and act as a dissipative reservoir. They may belong to the molecular wire or, if present, to a surrounding solvent. The respective coupling Hamiltonian is used in the form

$$H_{\text{S-R}} = \sum_m \ W_m(Q,Z)|\varphi_m\rangle\langle\varphi_m|. \tag{6}$$

The restriction to only diagonal contributions with respect to the electronic states in $H_{\text{S-R}}$ represents an additional assumption.

The model specified so far seems relatively simple if reduced to its electronic DOF. However, it will be demonstrated below that the use of delocalized electronic eigenstates of the wire (adiabatic states) extended to the respective potential-energy surface is just a very appropriate description for inelastic electron transfer through the wire. Note also that this is the natural way to consider what is known as the polaron picture of transport. Furthermore, the separation of the vibrational DOF into an active set and a set of reservoir modes has the great advantage to directly model vibrational energy redistribution and to include final lifetimes of vibrational states. In the description explained below these processes are restricted to a given electronic state. But the inclusion of nonadiabatic couplings may extend the pure intrastate inelastic processes by intrastate contributions. However, this is not a subject of the present studies and will be postponed to future activities.

A. Reduced density operator equations

As already explained our approach is based on the introduction of an *active* electron-vibrational system coupled to a *passive* system of reservoir (bath) DOF. Therefore, we have to utilize the methods of dissipative quantum dynamics.[31,34,35] The central quantity is the reduced density operator

$$\hat{\rho}(t)=\text{tr}_{\text{R}}\{\hat{W}(t)\}, \tag{7}$$

which is obtained from the complete statistical operator $\hat{W}(t)$ via a trace operation restricted to the reservoir states. Then the total population realized in the electronic state φ_m follows as

$$P_m(t)=\text{tr}_{\text{vib}}\{\langle\varphi_m|\hat{\rho}(t)|\varphi_m\rangle\}. \tag{8}$$

The equation of motion for $\hat{\rho}$ reads (see, e.g., Ref. 31)

$$\frac{\partial}{\partial t}\hat{\rho}(t)=-i\mathcal{L}\hat{\rho}(t). \tag{9}$$

Here, the Liouville superoperator $\mathcal{L}$ accounts for dissipation, too. We use a separation into a zero−order part and a coupling contribution according to

$$\mathcal{L}=\mathcal{L}_0+\mathcal{L}_V. \tag{10}$$

The coupling contribution comprises the wire-electrode coupling Eq. (4),

$$\mathcal{L}_V=\frac{1}{\hbar}(H_{\text{el-wire}}\ldots)_-, \tag{11}$$

whereas the zero-order part reads

$$\mathcal{L}_0=\frac{1}{\hbar}(H_{\text{wire}}+H_L+H_R\ldots)_- -i\mathcal{D}. \tag{12}$$

It is given by the wire Hamiltonian Eq. (2) and the electrode Hamiltonian Eq. (3). The superoperator $\mathcal{D}$ accounts for dissipation. According to the introduced model of the coupling to an environment, Eq. (6), dissipation proceeds as an intraelectronic state vibrational relaxation. Details on the structure of $\mathcal{D}$ can be found in Appendix A.

III. RATE EQUATION FOR THE ELECTRONIC STATE POPULATIONS

A. Some preliminary remarks

To underline the character of the results derived in the following parts of this paper we briefly recall those expressions which are more or less standard for the theoretical description of molecular wire conductivity.[15] Our description of electron transfer will end with rate equations governing the time dependence of the electronic state populations. These rate equations can be derived from the so-called generalized master equation (GME), (see, for example, Ref. 31) in the limit of short memory effects (in relation to the electron transfer time through the wire) and have the standard form

$$\frac{\partial}{\partial t}P_m=-\sum_{m\neq n}(k_{m\to n}P_m-k_{n\to m}P_n) \tag{13}$$

with rates $k_{m\to n}$ describing the transition from electronic state φ_m to φ_n. (Note also the remark in Appendix B1 on the fact that for a stationary situation the memory kernels automatically reduce to ordinary rate expressions.)

For the present example of a molecular wire embedded within two microelectrodes the following rates appear: the transfer rates into the wire $k_{L\to a}$, $k_{R\to a}$ and out of the wire $k_{a\to L}$, $k_{a\to R}$, the rates for intrawire transitions $k_{a\to b}$, and the rates $k_{L\to R}$ and $k_{R\to L}$ which directly interconnect both electrodes. In the language used to describe donor-acceptor electron transfer mediated by a molecular bridge the latter rates refer to the superexchange mechanisms whereas the other contributions are related to sequential processes. In a case where these sequential processes are of minor importance one can expect a current formula which is directly proportional to $k_{L\to R}-k_{R\to L}$. Otherwise one has to solve the complete set of rate equations (13). If the former-mentioned case can be provided the rate of forward transition reads

$$k_{L\to R}=\sum_{\mathbf{k},\mathbf{q}} f_{L\mathbf{k}}f_{R\mathbf{q}}k_{L\mathbf{k}\to R\mathbf{q}}, \tag{14}$$

with Fermi's *Golden Rule* expression $k_{L\mathbf{k}\to R\mathbf{q}}=2\pi|T_{L\mathbf{k},R\mathbf{q}}/\hbar|^2\ \delta(\omega_{L\mathbf{k}}-\omega_{R\mathbf{q}})$ for the rate, and the T matrix $T_{L\mathbf{k},R\mathbf{q}}$ of the left-right transition. The single-electron distribution reads for the left electrode

$$f_{L\mathbf{k}}=f_{\text{Fermi}}(\hbar\omega_{L\mathbf{k}}) \tag{15}$$

and

$$f_{R\mathbf{q}}=[1-f_{\text{Fermi}}(\hbar\omega_{R\mathbf{q}}-eV)] \tag{16}$$

for the right electrode. In both cases f_{Fermi} denotes the Fermi distribution. Such a single-electron approach is common in the literature (see, for example, Ref. 15) but has been criti-

cized on fundamental grounds[36] (cf. also the multielectron approach on electron tunneling through an array of quantum dots[37–39]).

Alternative notations of Eq. (14) have been presented in different ways. We mention the formula $k_{L\to R}=2\pi\int d\omega\, \mathrm{tr}_{\mathrm{el}}\{\hat{\Gamma}^{(R)}(\omega)\hat{G}(\omega)\hat{\Gamma}^{(L)}(\omega)\hat{G}^{+}(\omega)\}$ which has been adapted here to the scheme of Fig. 1.[12,13] The expression incorporates a trace with respect to all electronic states involved (those of the wire and the two electrodes). $\hat{G}$ denotes the (retarded) Green's operator of the wire (possibly including the interaction with the electrodes) and the operators $\hat{\Gamma}^{(L)}$ and $\hat{\Gamma}^{(R)}$ describe the coupling of the wire to the left and the right electrodes, respectively. Both are of second order in the wire-electrode coupling and include the density of electrode states Eq. (5) as well as the respective distribution functions, Eqs. (15) and (16). They read $\hat{\Gamma}^{(X)}(\omega)=\sum_{a,b}\Gamma^{(X)}_{ab}(\omega)|\varphi_a\rangle\langle\varphi_b|$ with the coupling rates ($f_{X\mathbf{k}}=f_X(\varepsilon_{X\mathbf{k}})$)

$$\Gamma^{(X)}_{ab}(\omega)=\frac{1}{\hbar^2}V_{aX}(\omega)V_{Xb}(\omega)\mathcal{N}_X(\omega)f_X(\omega). \tag{17}$$

In the most simple case the Green's operator is given as $\hat{G}(\omega)=\sum_a|\varphi_a\rangle\langle\varphi_a|/(\omega-\varepsilon_a+i\varepsilon)$ (note $\varepsilon\to+0$).

The introduction of the density of states of the left and right electrode and the use of frequency instead of wave-vector-dependent wire-electrode coupling matrix elements results in the alternative notation of the transfer rate

$$k_{L\to R}=\int d\Omega_l d\Omega_r \sum_{a,b}\Gamma^{(L)}_{ab}(\Omega_l)\mathcal{T}_{ab}(\Omega_l,\Omega_r)\Gamma^{(R)}_{ba}(\Omega_r), \tag{18}$$

which will be preferred in the following. The quantities $\mathcal{T}_{ab}(\Omega_l,\Omega_r)$ will be of central interest for the considerations in the whole paper. They describe the transmission of an electron through the wire which enters the wire with energy $\hbar\Omega_l$ (from the left electrode) and eventually changes its energy to $\hbar\Omega_r$ if leaving the wire (into the right electrode). Therefore we will name these quantities molecular wire *transmission coefficients*. How big the energy difference between the incoming and outgoing electron might be is directly regulated by the $\mathcal{T}_{ab}$.[40]

If the electronic wire levels are far away from the states of the electrode occupied initially and after the transmission process an easy derivation of the T matrix and the transmission coefficients becomes possible. Since any energetic resonance is absent between the electrodes and the wire levels the coupling between the wire and the left electrode only weakly disturbs the initial state of the electron transfer processes. Within first–order perturbation theory the states of the left electrode $|\varphi_{L\mathbf{k}}\rangle$ have to be extended by $\sum_b V_{L\mathbf{k},b}/\hbar(\varepsilon_{L\mathbf{k}}-\varepsilon_b)\times|\varphi_b\rangle$. Such a correction to the isolated electrode states results in an effective coupling matrix element between the states of the left and the right electrode which reads $V^{(\mathrm{eff})}_{L\mathbf{k},R\mathbf{q}}=\sum_b V_{L\mathbf{k},b}V_{b,R\mathbf{q}}/\hbar(\varepsilon_{L\mathbf{k}}-\varepsilon_b)$. This matrix element can be identified with $T_{L\mathbf{k},R\mathbf{q}}$ given in the Golden Rule formula from above and is known in electron transfer theory as the superexchange coupling matrix element.[31] The expression for the T matrix is easily converted into the following expressions for the transmission coefficients $\mathcal{T}_{ab}(\Omega_l,\Omega_r)=2\pi\delta(\Omega_r-\Omega_l)/|(\Omega_r-\varepsilon_a)(\Omega_l-\varepsilon_b)|$.

The given derivation asks for a generalization which accounts for vibrational DOF. To do this it only remains to replace the electronic state vectors and energies by respective combinations with vibrational contributions, i.e., we take the electron-vibrational states $\chi_{mM}\varphi_m$ (note that m comprises the wire states and those of both electrodes) and the energies $\varepsilon_m+\omega_{mM}$ (for the notation, see Sec. II). Moreover, the thermal distribution f_{th} of vibrational quanta is introduced extending the initial-state electron distribution given by the Fermi distribution of the left electrode. Then one directly obtains the transmission coefficient generalized to the incorporation of vibrational contributions:

$$\begin{aligned}\mathcal{T}_{ab}(\Omega_l,\Omega_r)=2\pi\sum_{M,N}&\delta(\Omega_r+\omega_M-\Omega_l-\omega_N)f_{\mathrm{th}}(\hbar\omega_N)\\&\times\sum_K\frac{\langle\chi_M|\chi_{aK}\rangle\langle\chi_{aK}|\chi_N\rangle}{|\Omega_r+\omega_M-\varepsilon_a-\omega_{aK}|}\\&\times\sum_L\frac{\langle\chi_N|\chi_{bL}\rangle\langle\chi_{bL}|\chi_M\rangle}{|\Omega_l+\omega_N-\varepsilon_b-\omega_{bL}|}.\end{aligned} \tag{19}$$

However, it is obvious that this formula does not give a complete description of the way electron-vibrational coupling affects the charge motion through the wire. According to its derivation the expression for $\mathcal{T}_{ab}$ is only valid if (i) the wire levels are far away from the electrode levels and (ii) if any vibrational relaxation is absent. It will be the task of all following considerations to present a formalism and to derive expressions which are of the type of Eq. (18) but remain valid also for the case of an energetic resonance between the wire levels and the electrode energies and account for vibrational relaxation.

B. Projection operator and general rate expression

From the earlier studies in Refs. 32 and 33 it is known how to derive rate equations of the type given in Eq. (13) together with rate expressions which do not contain any approximation with respect to the electron-vibrational coupling. To this end one has to construct equations of motion for the electronic state populations, Eq. (8). The populations can be deduced from the electron-vibrational (reduced) statistical operator $\hat{\rho}(t)$, Eq. (7), via the trace with respect to the vibrational DOF $\mathrm{tr}_{\mathrm{vib}}\{\ldots\}$ and via a matrix element given by the electronic state φ_m. It is a well-established technique to determine such a reduced quantity by introducing a projection superoperator $\mathcal{P}$. The superoperator achieves a separation of the reduced statistical operator $\hat{\rho}(t)$ of the electron-vibrational system into the sum of a time-dependent electronic part containing the state populations and into vibrational statistical operators $\hat{r}_m$. If applied to an arbitrary operator $\hat{O}$ the action of $\mathcal{P}$ follows as

$$\mathcal{P}\hat{O}=\sum_m \hat{r}_m\hat{\Pi}_m\mathrm{tr}\{\hat{\Pi}_m\hat{O}\}. \tag{20}$$

Here, tr{ . . . } denotes the trace with respect to the complete set of electron-vibrational states,

$$\hat{\Pi}_m = |\varphi_m\rangle\langle\varphi_m| \tag{21}$$

is the projector on the various electronic states, and the operators $\hat{r}_m$ refer to equilibrium states of the vibrational DOF which are realized if the respective electronic states φ_m have been occupied, i.e.,

$$\hat{r}_a = \exp(-H_a/k_BT)/\mathrm{tr}_{\mathrm{vib}}\{\exp(-H_a/k_BT)\}$$

and

$$\hat{r}_{X\mathbf{k}} \equiv \hat{r}_{\mathrm{neu}} = \exp(-H_{\mathrm{neu}}/k_BT)/\mathrm{tr}_{\mathrm{vib}}\{\exp(-H_{\mathrm{neu}}/k_BT)\}.$$

According to Eq. (20) the application of $\mathcal{P}$ to the reduced statistical operator results in

$$\mathcal{P}\hat{\rho}(t) = \sum_m \hat{r}_m \hat{\Pi}_m P_m(t). \tag{22}$$

If we take the trace with respect to the vibrational DOF and chose the diagonal matrix element given by the state φ_m we get from Eq. (22) the electronic population, Eq. (8). In the same manner a respective equation of motion for P_m can be constructed. The equations of motion for the state populations in their most general form are known as GME's and represent rate equations which include memory effects. Once the latter are neglected ordinary rate equations of the type of Eq. (13) are obtained.

The GME for the state populations can be deduced from the Nakajima-Zwanzig identity for $\mathcal{P}\hat{\rho}(t)$. It is given in Appendix B, Eq. (B2), and represents an exact equation for $\mathcal{P}\hat{\rho}(t)$. Here, the only deviation from the standard case is given by the fact that the original equation of motion for $\hat{\rho}(t)$ already accounts for dissipation. In this manner vibrational energy relaxation and dephasing enters the rate expression to be derived. From the Nakajima–Zwanzig identity one gets the required GME by taking respective matrix elements (see Appendix B). As a byproduct an expression for the memory kernel of the GME follows. It is given in Eq. (B13) as a quantity defined in the frequency domain which accounts for the electron–vibrational coupling beyond any perturbation theory and which incorporates a perturbation series with respect to the wire-electrode coupling, Eq. (4). Taking the kernel at $\omega = 0$ the rates entering the ordinary rate equations, Eq. (13) are obtained.

For the following studies we concentrate on rate expressions up to the fourth order with respect to the wire-electrode coupling. This approximation does not consider electrode-induced wire-level renormalization but is sufficient for the present aim to underline the importance of electron-vibrational coupling. Therefore we take the zero-frequency limit of the exact kernel, Eq. (B13), and introduce a restriction up to the fourth order with respect to the wire-electrode coupling. It gives the transition rates as

$$k_{m\to n} = \int_0^\infty dt\, K_{nm}^{(2)}(t) + \int_0^\infty dt_1 dt_2 dt_3 K_{nm}^{(4)}(t_1,t_2,t_3), \tag{23}$$

with the second-order contribution

$$K_{nm}^{(2)}(t) = -\mathrm{tr}\{\hat{\Pi}_n \mathcal{L}_V \mathcal{U}_0(t) \mathcal{L}_V \mathcal{P}\hat{\Pi}_m\}, \tag{24}$$

and the fourth-order contribution

$$\begin{aligned} K_{nm}^{(4)}(t_1,t_2,t_3) &= \mathrm{tr}\{\hat{\Pi}_n \mathcal{L}_V \mathcal{U}_0(t_1) \mathcal{L}_V [\mathcal{U}_0(t_2) - \mathcal{P}] \\ &\quad \times \mathcal{L}_V \mathcal{U}_0(t_3) \mathcal{L}_V \mathcal{P}\hat{\Pi}_m\} \\ &= K_{nm}^{(4,\mathrm{nf})}(t_1,t_2,t_3) - \sum_k K_{nk}^{(2)}(t_1) K_{km}^{(2)}(t_3). \end{aligned} \tag{25}$$

Both expressions incorporate the change from the Green's superoperator defined in the frequency domain to the time-evolution superoperator $\mathcal{U}_0$ [cf. Eq. (B6)], which is defined via a complete neglect of the wire-electrode coupling. This coupling is characterized in the above expressions by the Liouville superoperator $\mathcal{L}_V$, Eq. (11). Note also that $\mathcal{P}\hat{\Pi}_m$ is identical with $\hat{r}_m \hat{\Pi}_m$ which represents the initial-state electron-vibrational density operator.

The separation of $K_{nm}^{(4)}$ into the nonfactorized part $K_{nm}^{(4,\mathrm{nf})}$ and into the factorized contributions $K_{nk}^{(2)} K_{km}^{(2)}$ results from the projector $\mathcal{P}$ combined with $\mathcal{U}_0(t_2)$. The appearance of the factorized part needs an additional comment. First it is important to underline that a description which is exclusively based on second-order rate expressions such as Eq. (24) provides a complete dephasing between the wire states and those of the electrodes. This results from the fast intraelectronic state relaxation compared to the electron transfer time. Higher-order rate expressions which are in the present description of higher order with respect to the wire–electrode coupling account for vibrational and electronic coherences between wire states and the electrode levels. At the same time, however, they partially account for vibrational relaxation. It will be shown below in more detail that it is the role of the factorized part $K_{nk}^{(2)} K_{km}^{(2)}$ to compensate these relaxational contributions to avoid double counting when solving the rate equations.

The rate kernels can be directly computed when carrying out the various commutators involved. But alternatively one can use a classification based on the so-called Liouville space pathway description introduced in Fig. 11 of Appendix B below. In the next section we will calculate the second–order rate expressions. Independent from their appearance in the GME they are necessary to compute the factorized part, Eq. (25), of the fourth-order rate. These calculations are followed by an detailed analysis of the fourth-order rate expressions.

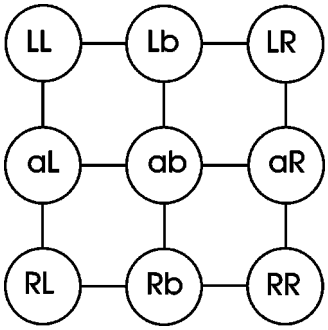

FIG. 3. Scheme of electronic density operator elements appearing in the fourth-order expression for the left-electrode-to-right-electrode transition. The transfer proceeds from the upper-left element LL to the lower-right element RR via all intermediate parts (for a detailed explanation, see Fig. 11 below).

IV. CALCULATION OF THE SECOND-ORDER RATE EXPRESSIONS

Taking the Liouville space pathway representation of the rate as given in Fig. 3 one first notices that within a second-order expression the rate $k_{L\mathbf{k}\to R\mathbf{q}}$ does not exist. There only exist $k_{L\mathbf{k}\to a}$ and $k_{a\to R\mathbf{q}}$. The respective rate kernels already introduced in Eq. (24) read in more detail (for $\tilde{U}_m$ see Appendix A)

$$K^{(2)}_{a,L\mathbf{k}}(t) = -\mathrm{tr}\{\hat{\Pi}_a \mathcal{L}_V \mathcal{U}_0(t) \mathcal{L}_V \hat{r}_{\mathrm{neu}} \hat{\Pi}_{L\mathbf{k}}\} = \frac{|V_{a,L\mathbf{k}}|^2}{\hbar^2} e^{-i(\varepsilon_{L\mathbf{k}}-\varepsilon_a)t} \mathrm{tr}_{\mathrm{vib}}\{\tilde{U}_{\mathrm{neu}}(t)\hat{r}_{\mathrm{neu}}\tilde{U}^+_a(t)\} + \mathrm{c.c.} \tag{26}$$

and

$$K^{(2)}_{R\mathbf{q},a}(t) = -\mathrm{tr}\{\hat{\Pi}_{R\mathbf{q}} \mathcal{L}_V \mathcal{U}_0(t) \mathcal{L}_V \hat{r}_{\mathrm{neu}} \hat{\Pi}_a\} = \frac{|V_{R\mathbf{q},a}|^2}{\hbar^2} e^{i(\varepsilon_{R\mathbf{q}}-\varepsilon_a)t} \mathrm{tr}_{\mathrm{vib}}\{\tilde{U}_a(t)\hat{r}_a\tilde{U}^+_{\mathrm{neu}}(t)\} + \mathrm{c.c.}, \tag{27}$$

In the second part of each expression we used Figs. 3 and 4 to simplify the trace expression. In particular, pathway II of Fig. 4 can be used to compute both trace expressions. The upper-left part of pathway II [from (LL) to (ab)] gives the expression for $K^{(2)}_{a,L\mathbf{k}}$ and the lower left [from (ab) to (RR)] that for $K^{(2)}_{R\mathbf{q},a}$. Both second-order kernels, Eqs. (26) and (27), contain the two different types of correlation functions (note the rearrangement of operators under the trace)

$$C_{\mathrm{neu},a}(t) = \mathrm{tr}_{\mathrm{vib}}\{\hat{r}_{\mathrm{neu}}\tilde{U}_{\mathrm{neu}}(t)\tilde{U}^+_a(t)\} \tag{28}$$

and

$$C_{a,\mathrm{neu}}(t) = \mathrm{tr}_{\mathrm{vib}}\{\hat{r}_a\tilde{U}_a(t)\tilde{U}^+_{\mathrm{neu}}(t)\}, \tag{29}$$

where the first index (a in the latter formula) indicates the electronic state to which the thermal equilibrium of the vibrational DOF refers (initial state of the transition). Noting Eq. (14) the complete rate expression of the second order reads [for $f_{L\mathbf{k}}$ see Eq. (15)]

$$k_{L\to a} = \sum_{\mathbf{k}} f_{L\mathbf{k}} \int_0^\infty dt\, K^{(2)}_{a,L\mathbf{k}}(t). \tag{30}$$

Instead of carrying out the $\mathbf{k}$ summation we introduce the density of states for the left-electrode levels, Eq. (5), and the coupling rate, Eq. (17). This results in the following representation of the rate:

$$k_{L\to a} = \int d\Omega_l \int_0^\infty dt\, \Gamma^{(L)}_{aa}(\Omega_l) e^{-i(\Omega_l-\varepsilon_a)t} C_{\mathrm{neu},a}(t) + \mathrm{c.c.} \tag{31}$$

In the same manner we obtain

$$k_{a\to R} = \int d\Omega_r \int_0^\infty dt\, \Gamma^{(R)}_{aa}(\Omega_r) e^{i(\Omega_r-\varepsilon_a)t} C_{a,\mathrm{neu}}(t) + \mathrm{c.c.}, \tag{32}$$

where all quantities involved are now defined for the right electrode.

Although both rate expressions are related to wire–electrode transitions they are common in electron transfer theory where they are usually termed nonadiabatic rates (see,

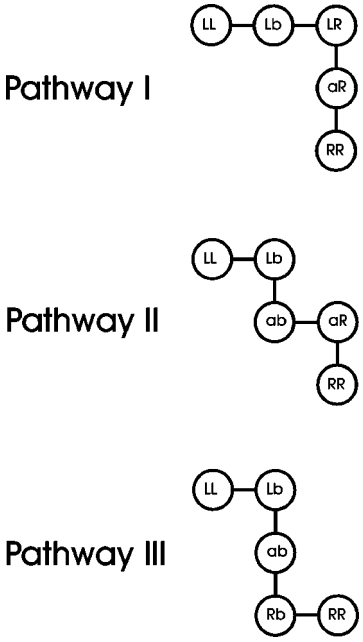

FIG. 4. Three different pathways of scheme in Fig. 3 corresponding to the left-electrode-to-right-electrode transition shown in Fig. 1. (There are three further pathways leading to complex-conjugate expressions of those shown in the figure.) Pathway I only incorporates intermediate density operators which are off diagonal with respect to the electronic states. This pathway may be related to what is known as the superexchange mechanism of electron transfer. Diagonal contributions appear in the middle of pathways II and III (element ab with $a=b$). They incorporate intraelectronic state vibrational relaxation.

e.g., Refs. 31 and 30). The only nonstandard item here is the incorporation of vibrational level broadening.

V. CALCULATION OF THE FOURTH-ORDER RATE EXPRESSION

For the following we will exclusively concentrate on the left-right-electrode transition. Of course fourth-order expressions also exist for the rates coupling the wire levels directly to the electrodes. However, their computation is outside the scope of this paper and will be discussed elsewhere.

The (nonfactorized) fourth-order kernel related to the transition rate $k_{L\to R}$ reads

$$K^{(4,\mathrm{nf})}_{R\mathbf{q},L\mathbf{k}}(t_1,t_2,t_3) = \mathrm{tr}\{\hat{\Pi}_{R\mathbf{q}}\mathcal{L}_V\mathcal{U}_0(t_1)\mathcal{L}_V\mathcal{U}_0(t_2)\mathcal{L}_V\mathcal{U}_0(t_3)\mathcal{L}_V\hat{r}_L\hat{\Pi}_{L\mathbf{k}}\}. \tag{33}$$

The various types of density operators appearing during the time evolutions contained in this kernel are shown in Fig. 3 within a two-dimensional scheme. One starts with the vibrational equilibrium in the left-electrode state $\varphi_{L\mathbf{k}}$ (described by $\hat{r}_L\hat{\Pi}_{L\mathbf{k}}$). According to the action of $\mathcal{L}_V$ the first or the second electronic quantum number changes. Thus after the time-evolution superoperator has been applied we may move in the scheme one position to the right with quantum numbers (Lb) or one position low with quantum numbers (aL). This procedure is continued up to arrival at the density operator diagonal in the quantum numbers $R\mathbf{q}$ of the right electrode. It is obvious that there exist six different ways which correspond to trace expressions being pairwise complex conjugated one to another. The three essentially different pathways are shown in Fig. 4.

The transition rate which connects the left with the right electrode is obtained from the fourth-order kernel, Eq. (25), as

$$k_{L\to R} = \sum_{\mathbf{k},\mathbf{q}} f_{L\mathbf{k}} f_{R\mathbf{q}} \int_0^\infty dt_1 dt_2 dt_3 K^{(4)}_{R\mathbf{q},L\mathbf{k}}(t_1,t_2,t_3). \tag{34}$$

It separates into a nonfactorized part and into factorized contributions formed by the second-order rate expressions.

Concentrating first on the nonfactorized part $K^{(4,\mathrm{nf})}_{R\mathbf{q},L\mathbf{k}}$ of the kernel one notices its decomposition into three terms related to the pathways I–III of Fig. 4. The part referring to pathway I only contains density operators that are off diagonal with respect to the electronic quantum numbers. This pathway describes the superexchange (tunneling) type of electron transfer,[33] whereas the terms related to pathways II and III account for a sequential type of transfer. Since for these pathways the intermediate density operator may become diagonal with respect to the electronic quantum numbers of the wire (see Fig. 4), intrawire-state vibrational relaxation takes place.

To calculate the nonfactorized part of $K^{(4)}_{R\mathbf{q},L\mathbf{k}}$ introduced in Eq. (34) we take Eq. (25) and note the pathways labeled I–III in Fig. 4. The notation follows the graphs of Fig. 11 below where we start from the initial density operator and put respective operators to the left as well as to the right. Remember that the electronic wire energies $\hbar\varepsilon_a$ have been split off from the time-evolution operators. We obtain

$$K^{(4,I)}_{R\mathbf{q},L\mathbf{k}}(t_1,t_2,t_3) = \frac{1}{\hbar^4}\sum_{a,b} \exp(-i\varepsilon_{L\mathbf{k}}(t_3+t_2)+i\varepsilon_{R\mathbf{q}}(t_2+t_1)-i\varepsilon_a t_1+i\varepsilon_b t_3) \times \mathrm{tr}_{\mathrm{vib}}\{V_{R\mathbf{q},a}\tilde{U}_a(t_1)V_{a,L\mathbf{k}}\tilde{U}_{\mathrm{neu}}(t_2)\tilde{U}_{\mathrm{neu}}(t_3)\hat{r}_{\mathrm{neu}}V_{L\mathbf{k},b}\tilde{U}^+_b(t_3)V_{b,R\mathbf{q}}\tilde{U}^+_{\mathrm{neu}}(t_2)\tilde{U}^+_{\mathrm{neu}}(t_1)\} + \mathrm{c.\,c.} \tag{35}$$

All transfer-matrix elements can be put outside the trace formula,

$$K^{(4,I)}_{R\mathbf{q},L\mathbf{k}}(t_1,t_2,t_3) = \frac{1}{\hbar^4}\sum_{a,b} V_{a,L\mathbf{k}}V_{L\mathbf{k},b}V_{b,R\mathbf{q}}V_{R\mathbf{q},a} \times \exp(i(\varepsilon_{R\mathbf{q}}-\varepsilon_a)t_1 - i(\varepsilon_{L\mathbf{k}}-\varepsilon_{R\mathbf{q}})t_2 - i(\varepsilon_{L\mathbf{k}}-\varepsilon_b)t_3)C^{(I)}_{ab}(t_1,t_2,t_3) + \mathrm{c.\,c.}, \tag{36}$$

and the trace expression results in a three-time correlation function which can be written as

$$C^{(I)}_{ab}(t_1,t_2,t_3) = \mathrm{tr}_{\mathrm{vib}}\{\tilde{U}_a(t_1)\tilde{U}_{\mathrm{neu}}(t_2+t_3)\hat{r}_{\mathrm{neu}}\tilde{U}^+_b(t_3) \times \tilde{U}^+_{\mathrm{neu}}(t_2+t_1)\}. \tag{37}$$

For practical reasons we do not give an arrangement of operators with the equilibrium statistical operator at the outer-left position. Furthermore, one should notice that the correlation function is labeled by the number of the Liouville space pathway to which the function belongs. The notation introduced in Eq. (36) shows that contributions of electronic and vibrational states to the complete rates could be separated. In particular, neglecting the influence of vibrational DOF means to replace $C^{(I)}_{ab}$ by 1.

Next we consider the kernel for the second pathway (see Fig. 4). In this case as well as in the case of the third pathway there exist an intermediate density operator which may be-

diagonal with respect to the wire states. In such a case the dissipation acts differently from the way it has been considered in pathway I [cf. Eq. (A5)] We obtain

$$K^{(4,II)}_{R\mathbf{q},L\mathbf{k}}(t_1,t_2,t_3)=\frac{1}{\hbar^4}\sum_{a,b}\exp(i(\varepsilon_{R\mathbf{q}}-\varepsilon_a)t_1-i(\varepsilon_a-\varepsilon_b)t_2 - i(\varepsilon_{L\mathbf{k}}-\varepsilon_b)t_3)\mathrm{tr}_{\mathrm{vib}}\{V_{R\mathbf{q},a}\tilde{U}_a(t_1)\mathcal{U}_{ab}(t_2) \times[V_{a,L\mathbf{k}}\tilde{U}_{\mathrm{neu}}(t_3)\hat{r}_{\mathrm{neu}}V_{L\mathbf{k},b}\tilde{U}^+_b(t_3)] \times V_{b,R\mathbf{q}}\tilde{U}^+_{\mathrm{neu}}(t_1)\}+\mathrm{c.\,c.} \quad (38)$$

If $a\neq b$ the time-evolution superoperator $\mathcal{U}_{ab}(t_2)$ reduces to the action of $\tilde{U}_a(t_2)$ from the left and $\tilde{U}^+_b(t_2)$ from the right. For $a=b$, however, the dissipative dynamics are more difficult to describe. In this case we will further write $\mathcal{U}_{aa}(t_2)$. Therefore we get

$$K^{(4,II)}_{R\mathbf{q},L\mathbf{k}}(t_1,t_2,t_3)=\frac{1}{\hbar^4}\sum_{a,b}V_{a,L\mathbf{k}}V_{L\mathbf{k},b}V_{b,R\mathbf{q}}V_{R\mathbf{q},a}\exp(i(\varepsilon_{R\mathbf{q}} -\varepsilon_a)t_1-i(\varepsilon_a-\varepsilon_b)t_2 - i(\varepsilon_{L\mathbf{k}}-\varepsilon_b)t_3)(\delta_{a,b}C^{(II)}_{aa}(t_1,t_2,t_3) +(1-\delta_{a,b})C^{(II,\mathrm{od})}_{ab}(t_1,t_2,t_3))+\mathrm{c.\,c.} \quad (39)$$

The off-diagonal (od) contribution reads similarly to $C^{(I)}_{ab}$, Eq. (37),

$$C^{(II,\mathrm{od})}_{ab}(t_1,t_2,t_3)=\mathrm{tr}_{\mathrm{vib}}\{\tilde{U}_a(t_1+t_2)\tilde{U}_{\mathrm{neu}}(t_3)\hat{r}_{\mathrm{neu}} \times\tilde{U}^+_b(t_3+t_2)\tilde{U}^+_{\mathrm{neu}}(t_1)\}, \quad (40)$$

however, the diagonal part follows as

$$C^{(II)}_{aa}(t_1,t_2,t_3)=\mathrm{tr}_{\mathrm{vib}}\{\tilde{U}_a(t_1)\mathcal{U}_{aa}(t_2) \times[\tilde{U}_{\mathrm{neu}}(t_3)\hat{r}_{\mathrm{neu}}\tilde{U}^+_a(t_3)]\tilde{U}^+_{\mathrm{neu}}(t_1)\}. \quad (41)$$

Its behavior will be discussed later on.

Finally we denote the expression for the third pathway,

$$K^{(4,III)}_{R\mathbf{q},L\mathbf{k}}(t_1,t_2,t_3)=\frac{1}{\hbar^4}\sum_{a,b}V_{a,L\mathbf{k}}V_{L\mathbf{k},b}V_{b,R\mathbf{q}}V_{R\mathbf{q},a} \times\exp(-i(\varepsilon_{R\mathbf{q}}-\varepsilon_b)t_1-i(\varepsilon_a-\varepsilon_b)t_2 - i(\varepsilon_{L\mathbf{k}}-\varepsilon_b)t_3)(\delta_{a,b}C^{(III)}_{aa}(t_1,t_2,t_3) +(1-\delta_{a,b})C^{(III,\mathrm{od})}_{ab}(t_1,t_2,t_3))+\mathrm{c.\,c.}, \quad (42)$$

with

$$C^{(III,\mathrm{od})}_{ab}(t_1,t_2,t_3)=\mathrm{tr}_{\mathrm{vib}}\{\tilde{U}_{\mathrm{neu}}(t_1)\tilde{U}_a(t_2)\tilde{U}_{\mathrm{neu}}(t_3)\hat{r}_{\mathrm{neu}} \times\tilde{U}^+_b(t_1+t_2+t_3)\}, \quad (43)$$

and with

$$C^{(III)}_{aa}(t_1,t_2,t_3)=\mathrm{tr}_{\mathrm{vib}}\{\tilde{U}_{\mathrm{neu}}(t_1)\mathcal{U}_{aa}(t_2) \times[\tilde{U}_{\mathrm{neu}}(t_3)\hat{r}_{\mathrm{neu}}\tilde{U}^+_a(t_3)]\tilde{U}^+_a(t_1)\}. \quad (44)$$

A more detailed computation of those correlation functions which are diagonal with respect to the electronic wire quantum numbers requires the use of the electron-vibrational state (energy) representation. Therefore we start to introduce this representation for the off-diagonal correlation functions in the next section.

Before doing this we note that there exist different approaches to handle the correlation functions related to the fourth-order kernel. An intensive study has been carried out for similar functions which one finds if calculating the third-order response functions for a model of two harmonic potential-energy surfaces coupled via an optical transition.[41] The restriction to two potential-energy surfaces constituted by a large set of harmonic oscillators allows to express all correlation functions via the spectral densities $J_{mn}(\omega)=\Sigma_j(g_m(j)-g_n(j))^2\ \delta(\omega-\omega_j)$. Here, $-2(g_m(j)-g_n(j))$ gives the (dimensionless) relative displacement of the vibrational equilibrium position if state φ_m or if state φ_n of the wire-electrode system is occupied. Such a representation via the spectral densities is particularly useful since experiments with ultrafast optical pulses give direct access to the time dependence of the correlation functions. This is different from the present study where the entire threefold time dependence is removed by integration.

A. Energy representation of the off-diagonal correlation functions

To introduce the electron-vibrational state representation we first give the expansion of $C^{(I)}_{ab}$, Eq. (37). After a rearrangement of the time-evolution operators in the trace expression one easily obtains [$f_{\mathrm{th}}(\hbar\omega)$ denotes the thermal distribution, for the definition of $\tilde{\omega}_{mM}$ see Eq. (A7)]

$$C^{(I)}_{ab}(t_1,t_2,t_3)=\sum_{K,L,M,N}f_{\mathrm{th}}(\hbar\omega_K)\mathrm{tr}_{\mathrm{vib}}\{\hat{\Pi}_K\hat{\Pi}_{bL}\hat{\Pi}_M\hat{\Pi}_{aN}\} \times\exp(-i(\tilde{\omega}_{aN}-\tilde{\omega}^*_M)t_1-i(\tilde{\omega}_K-\tilde{\omega}^*_M)t_2 - i(\tilde{\omega}_K-\tilde{\omega}^*_{bL})t_3). \quad (45)$$

The trace including projection operators on the various vibrational states abbreviates the respective product of vibrational overlap matrix elements (Franck-Condon factors). In the same manner one can rewrite the two remaining expressions, i.e., we get

$$C^{(II,\mathrm{od})}_{ab}(t_1,t_2,t_3)=\sum_{K,L,M,N}f_{\mathrm{th}}(\hbar\omega_K)\mathrm{tr}_{\mathrm{vib}}\{\hat{\Pi}_K\hat{\Pi}_{bL}\hat{\Pi}_M\hat{\Pi}_{aN}\} \times\exp(-i(\tilde{\omega}_{aN}-\tilde{\omega}^*_M)t_1-i(\tilde{\omega}_{aN}-\tilde{\omega}^*_{bL})t_2 - i(\tilde{\omega}_K-\tilde{\omega}^*_{bL})t_3) \quad (46)$$

and

$$C_{ab}^{(III,\mathrm{od})}(t_1,t_2,t_3)=\sum_{K,L,M,N} f_{\mathrm{th}}(\hbar\omega_K)\mathrm{tr}_{\mathrm{vib}}\{\hat{\Pi}_K\hat{\Pi}_{bL}\hat{\Pi}_M\hat{\Pi}_{aN}\}\times\exp(-i(\tilde{\omega}_M-\tilde{\omega}_{bL}^*)t_1-i(\tilde{\omega}_{aN}-\tilde{\omega}_{bL}^*)t_2-i(\tilde{\omega}_K-\tilde{\omega}_{bL}^*)t_3). \quad (47)$$

B. Energy representation of the diagonal correlation functions

$C_{aa}^{(II)}$ and $C_{aa}^{(III)}$ include vibrational relaxation within a single electronic wire state which may result in vibrational equilibrium within this state. Therefore, both trace expressions become independent of t_2 if this time argument becomes larger than a typical vibrational relaxation time. To demonstrate this we first consider the action of the time-evolution superoperator $\mathcal{U}_{aa}$. This is done by introducing the vibrational state representation already used in the foregoing section. We obtain

$$\mathcal{U}_{aa}(t_2)[\tilde{U}_{\mathrm{neu}}(t_3)\hat{r}_{\mathrm{neu}}\tilde{U}_a^+(t_3)]=\sum_{K,L} f(\hbar\omega_K)\exp(-i(\tilde{\omega}_K-\tilde{\omega}_{aL}^*)t_3)\langle\chi_K|\chi_{aL}\rangle\times\mathcal{U}_{aa}(t_2)[|\chi_K\rangle\langle\chi_{aL}|]. \quad (48)$$

To calculate the action of $\mathcal{U}_{aa}$ we reformulate $|\chi_K\rangle\langle\chi_{aL}|$ in such a manner that it corresponds to the initial value $\hat{\rho}(t_2=0;K;aL)$ of a density operator. Therefore we introduce $=|\chi_K\rangle\langle\chi_{aL}|/\mathrm{tr}_{\mathrm{vib}}\{|\chi_K\rangle\langle\chi_{aL}|\}$ which leads to

$$\hat{\rho}(t_2=0;K;aL)=\frac{|\chi_K\rangle\langle\chi_{aL}|}{\langle\chi_{aL}|\chi_K\rangle}. \quad (49)$$

Note that the dependence on the initial-state quantum numbers has been explicitly given. If one inserts this expression into Eq. (48) and lets t_2 go to infinity $\hat{\rho}(t_2;K;aL)$ changes to the equilibrium operator $\hat{r}_a$ and the K,L summation results in the correlation function $C_{\mathrm{neu},a}(t_3)$, Eq. (28). If inserted into $C_{aa}^{(II)}$, Eq. (41), the correlation function $C_{a,\mathrm{neu}}(t_1)$, Eq. (29), appears additionally. This indicates the possible compensation of the factorized part of the complete fourth-order kernel in the limit $t_2\to\infty$.

For further use, however, we also need the expressions for finite t_2 where this compensation is incomplete. Therefore the diagonal part $C_{aa}^{(II)}$ of the correlation function which belongs to the second Liouville space pathway is calculated in more detail. To do this we first give the state representation of $C_{aa}^{(II)}$, Eq. (41) [without calculating the action of $\mathcal{U}_{aa}(t_2)$ in detail],

$$C_{aa}^{(II)}(t_1,t_2,t_3)=\sum_{K,L,M,N,\bar{N}} f_{\mathrm{th}}(\hbar\omega_K)|\langle\chi_K|\chi_{aL}\rangle|^2\times\exp(-i(\tilde{\omega}_{aN}-\tilde{\omega}_M^*)t_1-i(\tilde{\omega}_K-\tilde{\omega}_{aL}^*)t_3)\langle\chi_M|\chi_{aN}\rangle\rho_{aN,a\bar{N}}\times(t_2;K;aL)\langle\chi_{a\bar{N}}|\chi_M\rangle. \quad (50)$$

Here we introduced the matrix elements $\rho_{aN,a\bar{N}}(t_2;K;aL)=\langle\chi_{aN}|\rho(t_2;K;aL))|\chi_{a\bar{N}}\rangle$ of the density operator, Eq. (49), if propagated to the finite time t_2. The initial condition reads

$$\rho_{aN,a\bar{N}}(t_2=0;K;aL)=\delta_{\bar{N},L}\left[\delta_{N,\bar{N}}+(1-\delta_{N,\bar{N}})\frac{\langle\chi_{aN}|\chi_K\rangle}{\langle\chi_{aL}|\chi_K\rangle}\right]. \quad (51)$$

The density matrix at finite t_2 is obtained in solving respective equations of motion which correspond to the time-evolution superoperator $\mathcal{U}_{aa}$. According to the relations introduced in Sec. II A we get

$$\frac{\partial}{\partial t}\rho_{aN,a\bar{N}}(t;K;aL)=-i(\tilde{\omega}_{aN}-\tilde{\omega}_{a\bar{N}}^*)\rho_{aN,a\bar{N}}(t;K;aL)+\delta_{N,\bar{N}}\sum_{\bar{K}}\Gamma_{a\bar{K}\to aN}\rho_{a\bar{K},a\bar{K}}(t;K;aL). \quad (52)$$

It separates into diagonal and off-diagonal contributions. The off-diagonal parts of the density matrix are simply determined whereas the diagonal part $P_{aN}(t)=\rho_{aN,aN}(t;K;aL)$ follows as the solution of a rate equation describing vibrational relaxation within the electronic state φ_a. We write

$$\rho_{aN,a\bar{N}}(t;K;aL)=\delta_{N,\bar{N}}P_{aN}(t;L)+(1-\delta_{N,\bar{N}})\rho_{aN,a\bar{N}}(t=0;K;aL)\times\exp(-i(\tilde{\omega}_{aN}-\tilde{\omega}_{a\bar{N}}^*)t). \quad (53)$$

Now, we can insert this expression into the correlation function, Eq. (50), to get

$$\begin{aligned}C_{aa}^{(II)}(t_1,t_2,t_3)=\sum_{K,L,M,N}&\times f_{\mathrm{th}}(\hbar\omega_K)\mathrm{tr}_{\mathrm{vib}}\{\hat{\Pi}_K\hat{\Pi}_{aL}\}\\&\times\exp(-i(\tilde{\omega}_K-\tilde{\omega}_{aL}^*)t_3)\\&\times P_{aN}(t_2;L)\mathrm{tr}_{\mathrm{vib}}\{\hat{\Pi}_M\hat{\Pi}_{aN}\}\\&\times\exp(-i(\tilde{\omega}_{aN}-\tilde{\omega}_M^*)t_1)\\&+(1-\delta_{L,N})f_{\mathrm{th}}(\hbar\omega_K)\mathrm{tr}_{\mathrm{vib}}\{\hat{\Pi}_K\hat{\Pi}_{aL}\hat{\Pi}_M\hat{\Pi}_{aN}\}\\&\times\exp(-i(\tilde{\omega}_{aN}-\tilde{\omega}_M^*)t_1-i(\tilde{\omega}_{aN}-\tilde{\omega}_{aL}^*)t_2\\&-i(\tilde{\omega}_K-\tilde{\omega}_{aL}^*)t_3).\end{aligned} \quad (54)$$

The first part of the fourfold summation cannot be separated into two double summations since the populations P_{aN} depend, via their initial values, on L. A separation is only valid in the limit $t_2=\infty$ where the initial value dependence vanishes. Nevertheless, we will denote this first part as $C_{aa}^{(\mathrm{f},II)}$ (factorized part) whereas the second part will read $C_{aa}^{(\mathrm{nf},II)}$ (nonfactorized part).

In the same manner as explained above we can also determine the diagonal part of the three-time correlation functions referring to the Liouville space pathway III. It differs

from $C_{aa}^{(II)}(t_1,t_2,t_3)$ only with respect to the t_1 dependence where $\tilde{\omega}_{aN}-\tilde{\omega}_M^*$ has to be replaced by $\tilde{\omega}_M-\tilde{\omega}_{aN}^*$. Again we will write $C_{aa}^{(III)}=C_{aa}^{(\mathrm{f},III)}+C_{aa}^{(\mathrm{nf},III)}$.

C. Complete fourth-order rate

According to the above discussions we separate the complete transmission coefficient into a nonfactorized and a factorized part. The first reads

$$\begin{aligned}\mathcal{T}_{ab}^{(\mathrm{nf})}(\Omega_l,\Omega_r)=\int_0^\infty dt_1dt_2dt_3\times[&(i(\Omega_r-\varepsilon_a)t_1-i(\Omega_l\\&-\Omega_r)t_2-i(\Omega_l-\varepsilon_b)t_3)C_{ab}^{(I)}(t_1,t_2,t_3)\\&+\exp(i(\Omega_r-\varepsilon_a)t_1-i(\varepsilon_a-\varepsilon_b)t_2\\&-i(\Omega_l-\varepsilon_b)t_3)(\delta_{a,b}C_{aa}^{(\mathrm{nf},II)}(t_1,t_2,t_3)\\&+(1-\delta_{a,b})C_{ab}^{(II,\mathrm{od})}(t_1,t_2,t_3))\\&+\exp(-i(\Omega_r-\varepsilon_b)t_1-i(\varepsilon_a-\varepsilon_b)t_2\\&-i(\Omega_l-\varepsilon_b)t_3)(\delta_{a,b}C_{aa}^{(\mathrm{nf},III)}(t_1,t_2,t_3)\\&+(1-\delta_{a,b})C_{ab}^{(III,\mathrm{od})}(t_1,t_2,t_3))]+\mathrm{c.c.}\end{aligned} \tag{55}$$

For the factorized part we get

$$\begin{aligned}\mathcal{T}_{aa}^{(\mathrm{f})}(\Omega_l,\Omega_r)=\int_0^\infty dt_1dt_2dt_3&\\\times\sum_{K,L,M,N}f_{\mathrm{th}}(\hbar\omega_K)&\mathrm{tr}_{\mathrm{vib}}\{\hat{\Pi}_K\hat{\Pi}_{aL}\}\\\times[\exp(-i(\Omega_l+\tilde{\omega}_K-\varepsilon_a-\tilde{\omega}_{aL}^*)t_3)+\mathrm{c.c.}]&\\\times[P_{aN}(t_2;L)-f_{\mathrm{th}}(\hbar\omega_{aN})]&\mathrm{tr}_{\mathrm{vib}}\{\hat{\Pi}_M\hat{\Pi}_{aN}\}\\\times[\exp(i(\Omega_r+\tilde{\omega}_M^*-\varepsilon_a-\tilde{\omega}_{aN})t_1)+\mathrm{c.c.}]&.\end{aligned} \tag{56}$$

If we neglect the vibrational contributions, the difference $P_{aN}(t_2;L)-f_{\mathrm{th}}(\hbar\omega_{aN})$ has to be set equal to zero. Hence, it is directly obvious that the factorized part of the transmission coefficient vanishes in the absence of electron-vibrational coupling.

Then, the final expression for the left-right transition rate can be cast into the following form:

$$\begin{aligned}k_{L\to R}=\int d\Omega_l d\Omega_r\mathrm{Re}\sum_{a,b}\Gamma_{ab}^{(L)}(\Omega_l)[&\mathcal{T}_{ab}^{(\mathrm{nf})}(\Omega_l,\Omega_r)\\&+\delta_{a,b}\mathcal{T}_{aa}^{(\mathrm{f})}(\Omega_l,\Omega_r)]\Gamma_{ba}^{(R)}(\Omega_r).\end{aligned} \tag{57}$$

The formula makes use of the electrode-wire coupling rates introduced in Eq. (17) and reads similarly to Eq. (18) where we already introduced the molecular wire transmission coefficients $\mathcal{T}_{ab}$. Here, this quantity has been separated into two parts. The parts $\mathcal{T}_{ab}^{(\mathrm{nf})}$ stem from the nonfactorized fourth-order kernel and are related to the contribution of pathway I as well as to the electronic off-diagonal contributions of pathways II and III. The second part of the transmission coefficients are diagonal with respect to the electronic quantum numbers of the wire and incorporate the electronic diagonal contributions of pathways II and III together with the contribution of the factorized part of the fourth-order kernel.

To carry out concrete computations based on Eq. (57) it remains to carry out the threefold time integration still appearing in the formulas for $\mathcal{T}^{(\mathrm{nf})}$ and $\mathcal{T}^{(\mathrm{f})}$. Accordingly the nonfactorized transmission coefficient takes the following form:

$$\begin{aligned}\mathcal{T}_{ab}^{(\mathrm{nf})}(\Omega_l,\Omega_r)=2i\sum_{K,M}&\frac{f_{\mathrm{th}}(\hbar\omega_K)}{[\Omega_r+\tilde{\omega}_M^*]-[\Omega_l+\tilde{\omega}_K]}\\&\times\sum_N\frac{\langle\chi_M|\hat{\Pi}_{aN}|\chi_K\rangle}{[\Omega_r+\tilde{\omega}_M^*]-[\varepsilon_a+\tilde{\omega}_{aN}]}\\&\times\sum_L\frac{\langle\chi_K|\hat{\Pi}_{bL}|\chi_M\rangle}{[\Omega_l+\tilde{\omega}_K]-[\varepsilon_b+\tilde{\omega}_{bL}^*]}\\&+2i\sum_{L,N}\frac{\delta_{a,b}(1-\delta_{L,N})+(1-\delta_{a,b})}{[\varepsilon_b+\tilde{\omega}_{bL}^*]-[\varepsilon_a+\tilde{\omega}_{aN}]}\\&\times\sum_K\frac{f_{\mathrm{th}}(\hbar\omega_K)\langle\chi_{aN}|\hat{\Pi}_K|\chi_{bL}\rangle}{[\Omega_l+\tilde{\omega}_K]-[\varepsilon_b+\tilde{\omega}_{bL}^*]}\\&\times\left\{\sum_M\frac{\langle\chi_{bL}|\hat{\Pi}_M|\chi_{aN}\rangle}{[\Omega_r+\tilde{\omega}_M^*]-[\varepsilon_a+\tilde{\omega}_{aN}]}\right.\\&\left.-\sum_M\frac{\langle\chi_{bL}|\hat{\Pi}_M|\chi_{aN}\rangle}{[\Omega_r+\tilde{\omega}_M]-[\varepsilon_b+\tilde{\omega}_{bL}^*]}\right\}.\end{aligned} \tag{58}$$

The various terms are arranged as follows. The first fourfold summation (with respect to the sets K, M, N, and L of vibrational quantum numbers) corresponds to pathway I of $K^{(4)}$, whereas the second fourfold summation relates to pathways II and III. The elimination of the term with $L=N$ in the part with $a=b$ indicates that the contribution describing vibrational relaxation has been removed. It will appear in $\mathcal{T}_{aa}^{(\mathrm{f})}$ (see below). To have a clear distinction between electronic and vibrational energies we arranged the wire energies, for example, as $\varepsilon_a+\tilde{\omega}_{aM}$. The vibrational contribution $\tilde{\omega}_{aM}$ is given by the complex quantity $\omega_{aM}-i\gamma_{aM}$, which includes beside the vibrational energies ω_{aM} the level broadening $\gamma_{aM}/2$ (cf. Appendix A). For both electrodes we set $\Omega_X+\tilde{\omega}_M$ $(X=L,R)$. The projection operators Π_{aN} (and others) enabled a compact notation of vibrational overlap integrals.

In a similar manner we may denote the factorized part of the transmission coefficient

$$\mathcal{T}^{(\mathrm{f})}_{aa}(\Omega_l,\Omega_r)=4\sum_{K,L} f_{\mathrm{th}}(\hbar\omega_K)|\langle\chi_K|\chi_{aL}\rangle \times\Bigg|^2\mathrm{Im}\frac{1}{[\Omega_l+\tilde{\omega}_K]-[\varepsilon_a-\tilde{\omega}^*_{aL}]} \times\sum_{M,N}\int_0^\infty dt_2[P_{aN}(t_2;L)-f_{\mathrm{th}}(\hbar\omega_{aN})]\Bigg| \times\langle\chi_M|\chi_{aN}\rangle|^2\mathrm{Im}\frac{1}{[\varepsilon_a+\tilde{\omega}_{aN}]-[\Omega_r+\tilde{\omega}^*_M]}. \tag{59}$$

The t_2 integral incorporates the (incomplete) compensation of those parts related to pathways II and III, including vibrational relaxation, and the factorized part of the total fourth-order rate kernel. The integral exists since the vibrational state population $P_{aN}(t_2;L)$ converges to the thermal distribution $f_{\mathrm{th}}(\hbar\omega_{aN})$ independently of the initial population of the vibrational level L.

The part of $\mathcal{T}^{(\mathrm{f})}_{aa}$ which is proportional to f_{th} follows from the product between the second-order transition rate from a left-electrode level into the wire and between the transition rate from the wire to a right-electrode level. Therefore, $\mathcal{T}^{(\mathrm{f})}_{aa}$ is responsible for the (incomplete) cancellation of the total incoherent (hoppinglike) processes of the electron transfer through the molecular wire as contained in the fourth order rate. Everything that is basically different from this incoherent transfer is contained in the transmission coefficient $\mathcal{T}^{(\mathrm{nf})}$, Eq. (58). The first part describes superexchange electron transfer since it looks similar to Eq. (19). This expression has been introduced as the generalization of the simple superexchange transmission coefficient to the inclusion of vibrational DOF [for a direct comparison with Eq. (19), interchange the vibrational quantum numbers N and K]. But $\mathcal{T}^{(\mathrm{nf})}$ includes vibrational level broadening since we included vibrational energy dissipation and dephasing. This ''generalized superexchange'' formula for the transmission coefficient is supplemented by additional terms which guarantee the validity of the formula not only for the case where the molecular wire states are far away from the Fermi sea but also where they are degenerated with it.

Although the derived formula gives a very general and complete description of the modification of the charge transmission through a molecular wire by vibrational DOF, there are some points that need to be mentioned. First, the approach is of fourth order with respect to the wire-electrode coupling. Therefore one cannot account for the modification of wire levels by the electrode-wire coupling. However, if vibrational motion and relaxation is fast enough higher orders of the electrode-wire coupling should be of less importance. This case of fast vibrational relaxation involves the described electron transfer mechanism of the type known in electron transfer literature as nonadiabatic transfer. However, the fourth-order rate realizes a deviation from the complete hoppinglike transfer through the wire. It accounts for coherence between the electrodes and the wire levels.

VI. SOME NUMERICAL ILLUSTRATIONS

To underline the importance of vibrational contributions we compute the transmission factors, Eqs. (58) and (59), as well as the current, Eq. (B8), for a sufficient simple model of a molecular wire. In doing so we may choose an arbitrary electronic wire spectrum. However, it seems more appropriate to consider the wire states of a tight-binding model with N_{mol} sites leading to the energy spectrum $\hbar\varepsilon_a=E_0+2V\cos a$ [$a=\pi\nu/(N_{\mathrm{mol}}+1)$ and $\nu=1,\ldots,N_{\mathrm{mol}}$]. The expansion coefficients of the wire states $|\varphi_a\rangle$ with respect to the site states read $c_a(m)=\sqrt{2/(N_{\mathrm{mol}}+1)}\sin(am)$. Furthermore, we will assume as already indicated in Fig. 1 that the first site of the wire couples to the left electrode and the last to the right electrode. (If the voltage drop appears at the right electrode the model for the wire levels remains valid at a finite applied voltage, too.)

The wire-electrode coupling matrix elements introduced in Eq. (4) follow as $V_{L\mathbf{k},a}=V_{L\mathbf{k},1}c_a(1)$ and $c^*_a(N_{\mathrm{mol}})V_{N_{\mathrm{mol}},R\mathbf{k}}$, which allow us to write $\Gamma^{(L)}_{ab}=c^*_a(1)c_b(1)\Gamma^{(L)}$ and $\Gamma^{(R)}_{ab}=c^*_a(N_{\mathrm{mol}})c_b(N_{\mathrm{mol}})\Gamma^{(R)}$. It is obvious that the newly introduced coupling rates are defined by the local wire-electrode interaction matrix elements. As a result we may write Eq. (57) as

$$k_{L\to R}=\int d\Omega_l d\Omega_r\Gamma^{(L)}(\Omega_l)\mathcal{T}(\Omega_l,\Omega_r)\Gamma^{(R)}(\Omega_r). \tag{60}$$

The total transmission coefficient separates into a nonfactorized part

$$\mathcal{T}^{(\mathrm{nf})}(\Omega_l,\Omega_r) =\mathrm{Re}\sum_{ab} c^*_a(1)c_b(1)\mathcal{T}^{(\mathrm{nf})}_{ab}(\Omega_l,\Omega_r)c^*_a(N_{\mathrm{mol}})c_b(N_{\mathrm{mol}}) \tag{61}$$

and into a factorized part

$$\mathcal{T}^{(\mathrm{f})}(\Omega_l,\Omega_r)=\mathrm{Re}\sum_a |c_a(1)c_a(N_{\mathrm{mol}})|^2\mathcal{T}^{(\mathrm{f})}_{aa}(\Omega_l,\Omega_r). \tag{62}$$

For the further discussion it is appropriate to additionally separate $\mathcal{T}^{(\mathrm{nf})}$ into $\mathcal{T}^{(\mathrm{sx})}$ corresponding to Liouville space pathway I (superexchange contribution, cf. Fig. 4) and into $\mathcal{T}^{(\mathrm{seq})}$ which refers to pathways II and III (sequential contribution).

Concentrating next on the potential-energy surface ΔU_a is seems to be sufficient to choose them all to be identical for the wire states. This assumption leads to the absence of any horizontal shifts of the ΔU_a one to another, and all the vibrational states χ_{aM} can be replaced by the single type $\chi_{\mathrm{exc}M}$, referring to the presence of the excess electron in the wire. Those states have to be confronted with the states $\chi_M\equiv\chi_{\mathrm{neu}M}$ of the neutral wire. In contrast to the many types of Franck-Condon overlap integrals appearing in Eqs. (58) and (59) there remains a single type, $f_{\mathrm{FC}}(M,N)=\langle\chi_{\mathrm{neu}M}|\chi_{\mathrm{exc}N}\rangle$ [note $\langle\chi_{\mathrm{exc}M}|\chi_{\mathrm{neu}N}\rangle=f^*_{\mathrm{FC}}(N,M)$, where in the case of harmonic-oscillator states the sign * can be removed]. Fur-

thermore, we will concentrate on one or two vibrational coordinates with vibrational energy

$$\omega_M = \sum_j M_j \omega_j , \tag{63}$$

leading to the reorganization energy

$$E_\lambda = \sum_j \hbar \omega_j [g_{\rm neu}(j) - g_{\rm exc}(j)]^2 . \tag{64}$$

To specify the level broadening we take an expression which corresponds to a (system-reservoir) coupling function linear in the reaction as well as the reservoir coordinates. Furthermore, the coupling function should be independent of the state of the wire (neutral or with the excess electron). Therefore, the used expression reads (see, e.g., Ref. 31)

$$\gamma_M = \sum_j [M_j(1+n(\omega_j)) + (1+M_j)n(\omega_j)]\gamma_j , \tag{65}$$

where n is the Bose-Einstein distribution and γ_j denotes a reference broadening.

As a result the ''superexchange'' part of the nonfactorized transmission coefficient, Eq. (61), reads

$$\begin{aligned}\mathcal{T}^{(\rm sx)}(\Omega_l,\Omega_r) = -2\,{\rm Im}\sum_{ab} c_a^*(1)c_b(1)c_b^*(N_{\rm mol})c_a(N_{\rm mol}) \\ \times \sum_{K,M} \frac{f_{\rm th}(\hbar\omega_K)}{\Omega_r - \Omega_l + \omega_M - \omega_K + i(\gamma_M+\gamma_K)} \\ \times \sum_N \frac{f_{\rm FC}(M,N) f_{\rm FC}(K,N)}{\Omega_r - \varepsilon_a + \omega_M - \omega_N + i(\gamma_M+\gamma_N)} \\ \times \sum_L \frac{f_{\rm FC}(K,L) f_{\rm FC}(M,L)}{\Omega_l - \varepsilon_b + \omega_K - \omega_L - i(\gamma_K+\gamma_L)} .\end{aligned} \tag{66}$$

For the ''sequential'' part we get

$$\begin{aligned}\mathcal{T}^{(\rm seq)}(\Omega_l,\Omega_r) = -2\,{\rm Im}\sum_{ab} c_a^*(1)c_b(1)c_b^*(N_{\rm mol})c_a(N_{\rm mol}) \\ \times \sum_{K,M} \frac{\delta_{a,b}(1-\delta_{K,M}) + (1-\delta_{a,b})}{\varepsilon_b - \varepsilon_a + \omega_M - \omega_K + i(\gamma_M+\gamma_K)} \\ \times \sum_N f_{\rm FC}(N,M) f_{\rm FC}(N,K) \\ \times \left\{ \frac{1}{\Omega_r - \varepsilon_a + \omega_N - \omega_K + i(\gamma_N+\gamma_K)} \right. \\ \left. - \frac{1}{\Omega_r - \varepsilon_b + \omega_N - \omega_M - i(\gamma_N+\gamma_M)} \right\} \\ \times \sum_L \frac{f_{\rm th}(\hbar\omega_L) f_{\rm FC}(L,K) f_{\rm FC}(L,M)}{\Omega_l - \varepsilon_b + \omega_L - \omega_M - i(\gamma_L+\gamma_M)} ,\end{aligned} \tag{67}$$

and the factorized part can be written as

$$\begin{aligned}\mathcal{T}^{(\rm f)}(\Omega_l,\Omega_r) = 4\sum_a |c_a(1)c_a(N_{\rm mol})|^2 \\ \times \sum_{K,L} {\rm Im}\frac{f_{\rm th}(\hbar\omega_K) f_{\rm FC}^2(K,L)}{\Omega_l - \varepsilon_a + \omega_K - \omega_L - i(\gamma_K+\gamma_L)} \\ \times \overline{\tau}_{\rm rel} \sum_{M,N} {\rm Im}\frac{(\delta_{L,N} - f_{\rm th}(\hbar\omega_N)) f_{\rm FC}^2(M,N)}{\Omega_r - \varepsilon_a + \omega_M - \omega_N - i(\gamma_M+\gamma_N)} .\end{aligned} \tag{68}$$

This formula, once it has been compared with Eq. (59), needs an additional comment. Instead of the t_2 integral containing the difference of the time-dependent vibrational state population and its asymptotic equilibrium value there appears $\overline{\tau}_{\rm rel}[\delta_{L,N} - f_{\rm th}(\hbar\omega_N)]$. This is an approximation of the exact expression and follows if one identifies $P_{aN}(t_2;L)$ in Eq. (59) with a simple exponentially decaying expression $P_{aN}(t_2=\infty;L) + [P_{aN}(t_2=0;L) - P_{aN}(t_2=\infty;L)] \times \exp(-t/\overline{\tau}_{\rm rel})$, with $P_{aN}(t_2=\infty;L) = f_{\rm th}(\hbar\omega_N)$ and $P_{aN}(t_2=0;L) = \delta_{N,L}$.

If the number of vibrational DOF is reduced to one or two reaction coordinates influencing the electron transfer in the entire wire, Eqs. (66)–(68), are ready for a direct numerical computation. It should be underlined here, however, that this is not the complicated formulation of the possible direct rate computation via a numerical propagation of the density matrix (feasible at least for the case of two vibrational DOF). Since we are interested in the time asymptotics (stationary case) this would be hardly accessible by a direct propagation (see e.g., Ref. 31).

A. Transmission coefficients

In the following, the parts $\mathcal{T}^{(\rm sx)}(\Omega_l,\Omega_r)$, $\mathcal{T}^{(\rm seq)}(\Omega_l,\Omega_r)$, and $\mathcal{T}^{(\rm f)}(\Omega_l,\Omega_r)$ of the total transmission coefficient $\mathcal{T} = \mathcal{T}^{(\rm sx)} + \mathcal{T}^{(\rm seq)} + \mathcal{T}^{(\rm f)}$ are presented as quantities depending on the energy $\hbar\Omega_l$ of the incoming electron (from the left electrode) and on the energy $\hbar\Omega_r$ of the outgoing electron (to the right electrode, see Fig. 5 as a first example). The transmission remains elastic if $\Omega_l = \Omega_r$. Such processes are contained in the $\Omega_l = \Omega_r$ stripe extending in the graphical representation of the transmission coefficients from the lower-left to the upper-right corner [see Fig. 5 and the following (Fig. 6); note that we use the term ''stripe'' instead of ''line'' to account for the lifetime broadening of all electron-vibrational levels]. The part of the Ω_l-Ω_r plane where $\Omega_l > \Omega_r$ (above the $\Omega_l = \Omega_r$ stripe) corresponds to transmission processes in which the incoming electron loses energy whereas it gains energy from the vibrational DOF for $\Omega_r > \Omega_l$ (below the $\Omega_l = \Omega_r$ stripe). The superexchange mechanism of electron transmission should dominate for $\Omega_l, \Omega_r \gg \omega_a$ whereas the sequential transfer would become of some importance if $\Omega_l, \Omega_r \approx \omega_a$. To have a proper graphical representation of the transmission coefficients the energy scale has been chosen in such a way that the energy E_0 (site energy of the wire elements) equals zero. The energy depen-

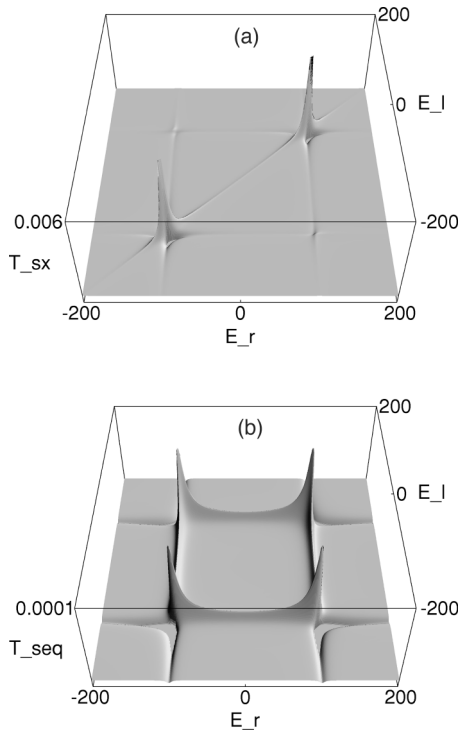

FIG. 5. Reference electron transmission coefficients of a molecular wire with two electronic levels versus the energy of the incoming electron $\hbar\Omega_l = E_l$ (from the left electrode), versus the energy of the outgoing electron $\hbar\Omega_r = E_r$ (into the right electrode), and for the absence of electron-vibrational coupling. E_l and E_r are given in meV and the transmission coefficients in $1/\text{meV}^3$. The parameters used for the calculations are $E_0 = 0$, $V = 100$ meV, $\hbar\omega_{\text{vib}} = 40$ meV, $\hbar\gamma_{\text{vib}} = 4$ meV, $\overline{\tau}_{\text{rel}} = 1/2\gamma_{\text{vib}}$, background line broadening is 2 meV, and $g_{\text{neu}} - g_{\text{exc}} = 0$. Room-temperature conditions have been chosen. (a) Superexchange part $\mathcal{T}^{(\text{sx})}$. (b) Sequential part $\mathcal{T}^{(\text{seq})}$ [note the different scale compared to $\mathcal{T}^{(\text{sx})}$].

dence of the coupling rates $\Gamma^{(L)}(\Omega_l)$ and $\Gamma^{(R)}(\Omega_r)$ will be responsible for those Ω_l-Ω_r regions which contribute to the total transition rate, Eq. (60). In this manner $\Gamma^{(L)}(\Omega_l)$ may define an upper limit for the energy of the incoming electron whereas $\Gamma^{(R)}(\Omega_r)$ fixes a lower limit for the energy of the outgoing electron. However, we will not consider this particular influence of the coupling rates but will analyze the whole Ω_l-Ω_r dependence of the transmission coefficients in drawing this quantity versus an appropriate part of the Ω_l-Ω_r plane.

The discussion will be carried out in two ways. First, to have a model which is simple enough to demonstrate the influence of the electron-vibration coupling we consider a two-level wire (stemming from a two-site system). Here, we can study how the vibrational parameters (electron-vibrational coupling strength, vibrational level broadening, vibrational frequency distribution) determine the different types of transmission coefficients. As a more realistic model a six-level wire model is used in a second part.

Figure 5 shows the superexchange contribution $\mathcal{T}^{(\text{sx})}$, Eq. (66), and the sequential contribution $\mathcal{T}^{(\text{seq})}$, Eq. (67), to the total transmission coefficient for the absence of any electron-vibrational coupling. This case is achieved if the displace-

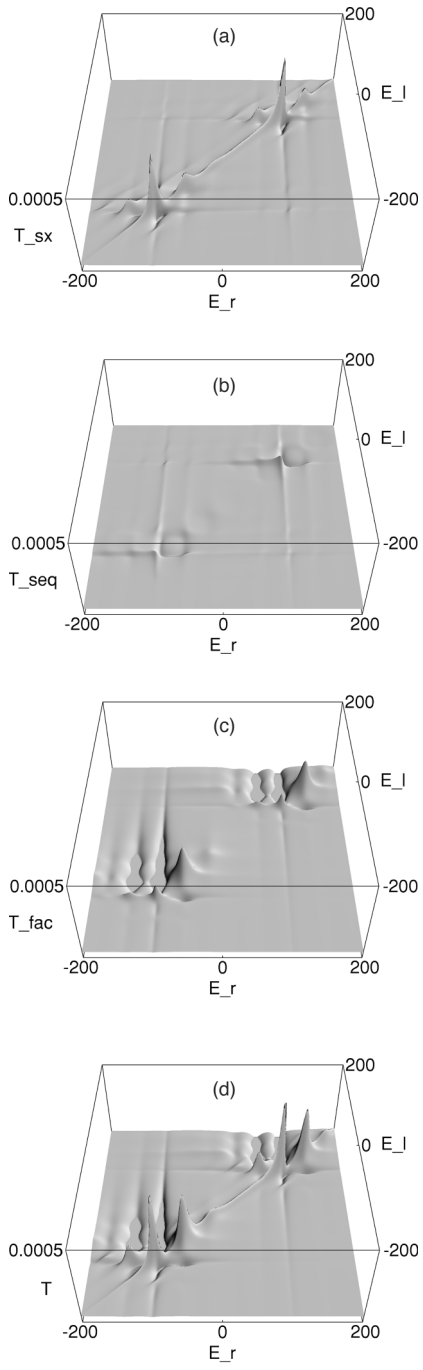

FIG. 6. Electron transmission coefficients of a molecular wire with two electronic levels modulated by a single vibrational coordinate versus the energy of the incoming electron $\hbar\Omega_l = E_l$ (from the left electrode) and versus the energy of the outgoing electron $\hbar\Omega_r = E_r$ (into the right electrode). E_l and E_r are given in meV and the transmission coefficients in $1/\text{meV}^3$. The parameters used for the calculations are $E_0 = 0$, $V = 100$ meV, $\hbar\omega_{\text{vib}} = 40$ meV, $\hbar\gamma_{\text{vib}} = 4$ meV, $\overline{\tau}_{\text{rel}} = 1/2\gamma_{\text{vib}}$, background line broadening is 2 meV, $g_{\text{neu}} - g_{\text{exc}} = 1$, and thermal energy is 1 meV. (a) Superexchange part $\mathcal{T}^{(\text{sx})}$. (b) Sequential part $\mathcal{T}^{(\text{seq})}$. (c) Factorized part $\mathcal{T}^{(\text{fac})}$. (d) Total transmission coefficient. (To compute the transmission coefficients, the inclusion of ten vibrational levels appeared to be sufficient.)

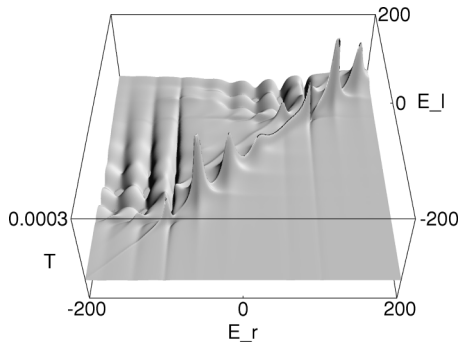

FIG. 7. Total electron transmission coefficient of a molecular wire with two electronic levels modulated by a single vibrational coordinate versus the energy of the incoming electron $\hbar\Omega_l = E_l$ (from the left electrode) and versus the energy of the outgoing electron $\hbar\Omega_r = E_r$ (into the right electrode). E_l and E_r are given in meV and the transmission coefficients in $1/\text{meV}^3$. The parameters used for the calculations are $E_0 = 0$, $V = 100$ meV, $\hbar\omega_{\text{vib}} = 40$ meV, $\hbar\gamma_{\text{vib}} = 4$ meV, $\bar{\tau}_{\text{rel}} = 1/2\gamma_{\text{vib}}$, background line broadening is 2 meV, $g_{\text{neu}} - g_{\text{exc}} = 1.5$, and thermal energy is 1 meV.

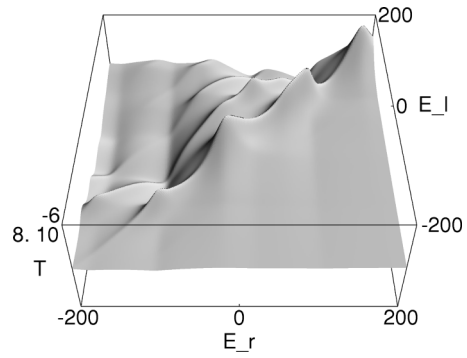

FIG. 8. Total electron transmission coefficient of a molecular wire with two electronic levels modulated by two vibrational coordinates versus the energy of the incoming electron $\hbar\Omega_l = E_l$ (from the left electrode) and versus the energy of the outgoing electron $\hbar\Omega_r = E_r$ (into the right electrode). E_l and E_r are given in meV and the transmission coefficients in $1/\text{meV}^3$. The parameters used for the calculations are $E_0 = 0$, $V = 100$ meV, low-frequency vibration $\hbar\omega_{\text{low}} = 8$ meV, high-frequency vibration $\hbar\omega_{\text{high}} = 80$ meV, level broadening equal for both modes, $\hbar\gamma_{\text{vib}} = 2$ meV, $\bar{\tau}_{\text{rel}} = 1/2\gamma_{\text{vib}}$, background line broadening is 1 meV, $g(\text{low})_{\text{neu}} - g(\text{low})_{\text{exc}} = 1.5$, $g(\text{high})_{\text{neu}} - g(\text{high})_{\text{exc}} = 1$, and thermal energy is 20 meV.

ments are removed between the PES belonging to the wire and those belonging to the electrodes ($g_{\text{neu}} = g_{\text{exc}}$ and thus $E_\lambda = 0$; all other parameters used in the calculation are given in the figure captions). As a result all vibrational overlap integrals reduce to Kronecker's δ function, but vibrational level broadening remains, resulting in the line broadening in the transmission factor. In particular, the transmission factor corresponding to the factorized part of the complete quantity vanishes [this can be easily clarified in writing Eq. (68) for $g_{\text{neu}} = g_{\text{exc}}$]. In contrast, $\mathcal{T}^{(\text{sx})}$ shows for $\Omega_l = \Omega_r$ two peaks corresponding to the two wire levels. The same behavior is obtained for $\mathcal{T}^{(\text{seq})}$ shown in Fig. 5(b). But there are two additional peaks for $\Omega_l \neq \Omega_r$ following from inelastic transitions caused by the coupling to the environmental DOF. Once this coupling is removed (vanishing vibrational level broadening) all these peaks disappear which can be easily confirmed by an analysis of Eq. (67). Note also that $\mathcal{T}^{(\text{seq})}$ shown in Fig. 5 is nearly two orders-of-magnitude smaller than $\mathcal{T}^{(\text{sx})}$. As expected, $\mathcal{T}^{(\text{sx})}$ dominates the transmission coefficient if the electron-vibrational coupling is absent.

Like in Fig. 5 we will also observe in the following figures regions in the Ω_l-Ω_r plane where the complete transmission coefficient becomes negative. Although these negative contributions may be compensated once the total rate, Eq. (60), has been calculated, they indicate an ill-defined rate expression. But it is well known how to overcome this problem (see, e.g., Refs. 33 and 45). Instead of calculating rate expressions one has to determine the complete memory kernel of the GME, Eq. (B3), which now has to be used to determine the electronic level populations. (The importance of an improved iteration of the rate expressions has been also underlined in Ref. 45.) In particular, the possible importance of memory effects indicates that electron-vibrational coherence is present, and, following from this, that the electron-vibrational dynamics proceed in a region beyond a pure hopping transfer.

The influence of the coupling to a single vibrational mode is shown in Fig. 6. For the chosen value of the electron-vibrational coupling strength (reorganization energy is 0.04 eV) the superexchange part of $\mathcal{T}$ is reduced by one order of magnitude compared to the case of vanishing electron-vibrational coupling but shows a reacher structure in the Ω_l-Ω_r plane. And the sequential and factorized parts become of some importance. If the electron-vibrational coupling is further increased all transmission coefficients are reduced additionally as demonstrated in Fig. 7. For the considered example the reorganization energy, Eq. (64), amounts to 0.09 eV and the transmission coefficient shows different vibrational satellites of the two main peaks. They are positioned not only on the $\Omega_l = \Omega_r$ stripe but also outside, demonstrat-

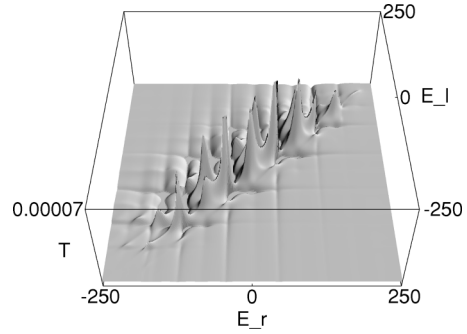

FIG. 9. Total electron transmission coefficient of a molecular wire with six electronic levels modulated by a single vibrational coordinate versus the energy of the incoming electron $\hbar\Omega_l = E_l$ (from the left electrode) and versus the energy of the outgoing electron $\hbar\Omega_r = E_r$ (into the right electrode). E_l and E_r are given in meV and the transmission coefficients in $1/\text{meV}^3$. The parameters used for the calculations are $E_0 = 0$, $V = 100$ meV, $\hbar\omega_{\text{vib}} = 40$ meV, $\hbar\gamma_{\text{vib}} = 4$ meV, $\bar{\tau}_{\text{rel}} = 1/2\gamma_{\text{vib}}$, background line broadening is 2 meV, $g_{\text{neu}} - g_{\text{exc}} = 1$, and thermal energy is 1 meV.

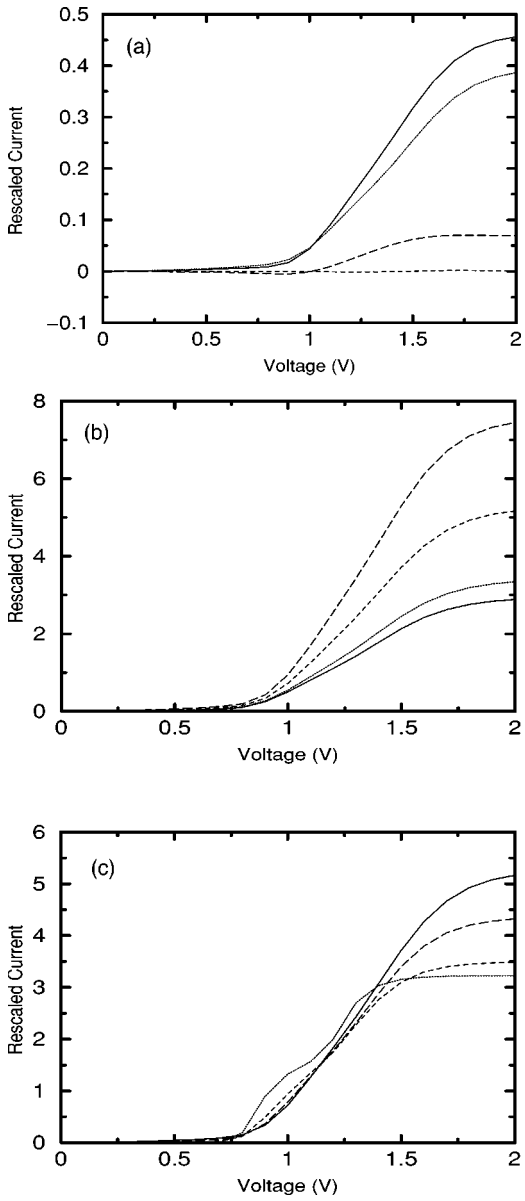

FIG. 10. Current-voltage characteristics of the wire discussed in Fig. 7 (the case of symmetrically applied voltage; E_0 has been taken 0.5 eV above the Fermi edge in the unbiased case). (a) Fourth-order reduced current according to Eq. (70) (full line, $\hbar\gamma_{\rm vib}=8$ meV, $g_{\rm neu}-g_{\rm exc}=2$, all other parameters as in Fig. 7), ''superexchange'' contribution $j^{(\rm sx)}$ (dashed line), ''sequential'' contribution $j^{(\rm seq)}$ (long-dashed line), and ''factorized'' contribution $j^{(\rm f)}$ (dotted line). (b) Reduced second-order current $I/e\Gamma_0$ (full line) and reduced total current $I/e\Gamma_0$ according to Eq. (69) [long-dashed line: $\hbar\Gamma_0=10$ meV, dashed line: $\hbar\Gamma_0=5$ meV, dotted line: $\hbar\Gamma_0=1$ meV, all other parameters as in (a)]. (c) Reduced total current $I/e\Gamma_0$ according to Eq. (69) [$\hbar\Gamma_0=5$ meV; full line: $g_{\rm neu}-g_{\rm exc}=2$ ($E_\lambda=160$ meV); long-dashed line: $g_{\rm neu}-g_{\rm exc}=1.8$ ($E_\lambda=130$ meV), dashed line: $g_{\rm neu}-g_{\rm exc}=1.5$ ($E_\lambda=90$ meV); dotted line: $g_{\rm neu}-g_{\rm exc}=1$ ($E_\lambda=40$ meV), all other parameters as in part (a)].

ing the importance of inelastic electron transmission channels.[42] Obviously the satellite structure becomes more complex if the transferred electron is coupled to two vibrational modes as can be seen in Fig. 8. A somewhat more realistic wire model is used in Fig. 9 showing the transmission coefficient for a six-level wire.

All given examples demonstrate the capability of the chosen approach to compute the left–right electron transmission rate $k_{L\to R}$, and they underlined the importance of an inelastic electron transmission. The influence of these inelastic contributions on a IV characteristic of a molecular wire are demonstrated in the last part.

B. Current-voltage characteristics

As a first application of the formalism presented so far we compute the current-voltage characteristics for the reference case of a two-site wire modulated by a single vibrational coordinate and in the presence of a symmetrically applied voltage (the wire levels stay at their zero-bias position). Since we are mainly interested in effects originated by the vibrational coordinate it suffices for the following to reduce the frequency dependence of the coupling rates [cf. Eq. (60)] to that of the Fermi distribution, i.e., we set $\Gamma^{(X)}(\omega)=\Gamma_0 f_X(\omega)$ where $\Gamma_0=|V/\hbar|^2\mathcal{N}$ depends on the constant transfer-matrix element V and the constant electrode density of states $\mathcal{N}$ (remember also the neglect of wire-level renormalization due to the presence of the electrode states).

If the approximation taken for $\Gamma^{(X)}(\omega)$ is also introduced into the second-order rate expressions the entire current follows as [cf. Eq. (B8)]

$$I/e\Gamma_0=j^{(II)}+\Gamma_0 j^{(IV)}. \tag{69}$$

$j^{(II)}$ denotes the expression which is obtained from second-order electrode-wire coupling contributions. It is easily derived when using the formulas of Sec. IV [and Eq. (B8)]. The fourth-order reduced current $j^{(IV)}$ reads

$$\begin{aligned} j^{(IV)}=\int d\Omega_1 d\Omega_2 \mathcal{I}(\Omega_1,\Omega_2)\{&f_{\rm Fermi}(\hbar\Omega_1-eV/2)\\ &\times[1-f_{\rm Fermi}(\hbar\Omega_2+eV/2)]-f_{\rm Fermi}(\hbar\Omega_1+eV/2)\\ &\times[1-f_{\rm Fermi}(\hbar\Omega_2-eV/2)]\}. \end{aligned} \tag{70}$$

According to the separation of the transmission coefficient into the various contributions, Eqs. (66)–(68), the fourth-order current can be split into the ''superexchange,'' the ''sequential,'' and the ''factorized'' contributions $j^{(\rm sx)}$, $j^{(\rm seq)}$, and $j^{(\rm f)}$, respectively. Their dependence on the (symmetrically) applied voltage is shown in Fig. 10(a). The parameters used refer to the transmission coefficients presented in Fig. 7. However, a somewhat larger vibrational level broadening and a larger reorganization energy has been taken. Moreover, the factorized part of the fourth-order transmission coefficient, Eq. (59), is determined in solving numerically the rate equation for the vibrational level populations $P_{aN}(t)$. Even this factorized part $j^{(\rm f)}$ dominates the total fourth-order current, although the superexchange contribution should be favored since up to a bias of 0.8 V the wire levels are out of resonance with the occupied electrode levels.

The voltage dependence of the second-order contribution $j^{(II)}$ can be found in Fig. 10(b). To get the total (reduced) current $I/e\Gamma_0$, Eq. (69), we have to fix the quantity $\hbar\Gamma_0$ to a

range less than 10 meV.[43] As can be seen just in this weak electrode–wire coupling case the second-order contribution is remarkablly modified by the fourth-order one. A detailed inspection of the way $j^{(II)}$ and $j^{(IV)}$ are influenced by the electron-vibrational coupling indicates the dominance of the fourth-order contribution. Finally, for the intermediate value $\hbar\Gamma_0 = 5$ meV the total current is drawn in Fig. 10(c) dependent on the electron-vibrational coupling strength. The increase of the current with an increase of the electron-vibrational coupling for the range of resonant transitions from the left electrode into the wire levels is obvious.

VII. CONCLUSIONS

A comprehensive theory of inelastic electron transmission through molecular wires has been offered in the present paper. The description is based on a consequent inclusion of the electron-vibrational coupling, considers vibrational energy relaxation and dephasing, and accounts for coherence in the course of the transfer. The theory ends up with a rate equation (possibly including memory effects) for those electronic state populations which are of relevance for the electron transmission. Since the rate expressions are given as a power expansion with respect to the wire–electrode coupling the description is beyond a simple ''Golden Rule'' approach. Calculating the electrode-wire-electrode transfer rate in the fourth order with respect to the wire-electrode coupling allows to generalize standard expressions for the wire transmission rate to the inclusion of inelastic-scattering events at the vibrational quanta of the wire. On one hand, there appears a simple modification of the pure electronic rate formula by augmenting the involved electronic levels via the addition of the vibrational level manifold. But there are further contributions to the rate which guarantee the validity of the rate formula also when the wire levels come into resonance with the electrode levels. All contributions to the transfer rate could by classified via the so-called Liouville space pathways. The feasibility of the approach could be demonstrated by some first calculations of current-voltage characteristics concentrated in a two-level wire and a symmetrically applied voltage. And indeed, a pronounced increase of the current with an increase of the electron-vibrational coupling has been found.

Although the presented numerical calculations are restricted to the case of a single and of two vibrational coordinates the approach may account for an arbitrary large number (if the three-time correlation functions are calculated using the spectral densities of the vibrational coordinates). Furthermore, the description can directly be tied to quantum chemical calculations of the adiabatic wire levels and on respective potential-energy surfaces. And as a third directly possible extension we refer to a renunciation of the simple model of a symmetrically applied voltage. More involved descriptions are known which, already on the level of the used simple tight-binding description of the wire, may allow for a self-consistent formulation of the voltage drop across the wire.[17] (All these questions are undergoing study and results will be published in the near future.)

Of more basic importance would be the inclusion of the wire-level renormalization due to the wire-electrode coupling. In fact it becomes possible to combine the very efficient projection operator approach which accounts for electron-vibrational couplings with infinite-order considerations of the wire-electrode coupling.[29] Such considerations will extend considerably the validity of the approach given here.

ACKNOWLEDGMENTS

Illuminative discussions with E. G. Petrov and P. Hänggi are gratefully acknowledged.

APPENDIX A: DISSIPATIVE PART OF THE DENSITY OPERATOR EQUATIONS

In the following a detailed expression for the dissipative superoperator $\mathcal{D}$ introduced in Eq. (12) will be given. To simplify the considerations and since details of vibrational relaxation are of less importance for the considerations in this paper we apply the well-known secular approximation which in operator notation is given by the so-called Lindblad type of dissipative superoperator (see, for example, Ref. 44)

$$-\mathcal{D}\hat{\rho} = -\sum_A \{\tfrac{1}{2}(L_A L_A^+, \hat{\rho})_+ - L_A^+ \hat{\rho} L_A\}. \tag{A1}$$

The new operators read $L_A^+ = l^+_{mM\to mN}\hat{\Pi}_m$ with the projector on the electronic states $\hat{\Pi}_m$, Eq. (21) (remember that m covers all involved electronic levels), and with $l^+_{mM\to mN} = \sqrt{\Gamma_{mM\to mN}}|\chi_{mN}\rangle\langle\chi_{mM}|$. The latter quantity generates transitions from the vibrational state χ_{mM} to the state χ_{mN}. How to compute the respective transition rate $\Gamma_{mM\to mN}$ has been well documented in the literature and should not be repeated here (see, e.g., Ref. 31). For further purposes we introduce $\hat{\gamma}_m = \Sigma_{M,N} l_{mM\to mN} l^+_{mM\to mN}$ which becomes identical to

$$\hat{\gamma}_m = \sum_M 2\gamma_{mM}|\chi_{mM}\rangle\langle\chi_{mM}| \tag{A2}$$

with the electron-vibrational level broadening (inverse lifetime) $\gamma_{mM} = \Sigma_N \Gamma_{mM\to mN}/2$. Accordingly the dissipative part of the density operator equation is written as

$$-\mathcal{D}\hat{\rho} = -\left(\tfrac{1}{2}\sum_m \hat{\gamma}_m\hat{\Pi}_m, \hat{\rho}\right)_+ + \sum_m \sum_{M,N} l^+_{mM\to mN}\hat{\Pi}_m\hat{\rho}(t)\hat{\Pi}_m l_{mM\to mN}. \tag{A3}$$

In Sec. V we need the solution of the density operator equation exclusively defined by $\mathcal{L}_0$, Eq. (12). It can be formally written as

$$\hat{\rho}(t) = \mathcal{U}_0(t,t_0)\hat{\rho}(t_0), \tag{A4}$$

where the time-evolution superoperator $\mathcal{U}_0$ has been introduced. Taking the matrix elements $\hat{\rho}_{mn} = \langle\varphi_m|\hat{\rho}|\varphi_n\rangle$, which just define operators in the state space of the active vibrational coordinates, we may write

$$\hat{\rho}(t)=\mathcal{U}_0(t,t_0)\sum_{m,n}\hat{\rho}_{mn}(t_0)|\varphi_m\rangle\langle\varphi_n|$$

$$=\sum_{n,m}|\varphi_m\rangle\langle\varphi_n|[\delta_{m,n}\mathcal{U}_{mm}(t,t_0)\hat{\rho}_{mm}(t_0)+(1-\delta_{m,n})$$

$$\times\tilde{U}_m(t-t_0)\hat{\rho}_{mn}(t_0)\tilde{U}_n^{+}(t-t_0)]. \tag{A5}$$

The time propagation of the density operator differs depending on the concrete type of matrix elements, i.e., if the diagonal or off-diagonal elements are affected. $\mathcal{U}_{mm}$ solves the vibrational density operator equation diagonal in the electronic quantum number whereas $\tilde{U}_m$ generates the time propagation of the off-diagonal elements. It is given as a generalized time-evolution operator including dissipation

$$\tilde{U}_m(t)=\exp\left(-\frac{i}{\hbar}\left(\hbar\omega_m+H_m-\frac{i\hbar}{2}\hat{\gamma}_m\right)t\right). \tag{A6}$$

For further use we will split off the part including ε_m, write $\exp(-\varepsilon_m t)\tilde{U}_m(t)$ instead of $\tilde{U}_m(t)$, and introduce

$$\tilde{\omega}_{mM}=\omega_{mM}-i\gamma_{mM}. \tag{A7}$$

Once $\tilde{U}_m(t)$ has been expanded with respect to the vibrational eigenstates of H_m it simply reads $\tilde{U}_m(t)=\Sigma_M\exp(-i\tilde{\omega}_{mM}t)\,|\chi_{mM}\rangle\langle\chi_{mM}|$.

APPENDIX B: THE GME FOR THE STATE POPULATIONS

According to the projection operator approach briefly explained in Sec. III B we give here some details on the derivation of a GME valid for the total electronic level populations. It is based on the equation of motion (9) for the reduced density operator, Eq. (7), of the electron-vibrational system.

In a first step we will derive the Nakajima-Zwanzig identity for $\mathcal{P}\hat{\rho}$, where $\mathcal{P}$ denotes the projection superoperator defined in Eq. (20). The introduction of $\mathcal{P}$ and the orthogonal complement, $\mathcal{Q}=1-\mathcal{P}$, into the density operator Eq. (9) leads to a separation into two equations, one obeyed by $\mathcal{P}\hat{\rho}$ and one by $\mathcal{Q}\hat{\rho}$. Taking the solution of the equation for $\mathcal{Q}\hat{\rho}$ including the assumption $\mathcal{Q}\hat{\rho}(t_0)=0$ and introducing the time-propagation superoperator

$$\mathcal{U}(t)=\exp\{-i\mathcal{Q}\mathcal{L}t\}, \tag{B1}$$

a closed equation for $\mathcal{P}\hat{\rho}$ results (Nakajima-Zwanzig identity):

$$\frac{\partial}{\partial t}\mathcal{P}\hat{\rho}(t)=-i\mathcal{P}\mathcal{L}\mathcal{P}\hat{\rho}(t)-\int_{t_0}^{t}d\bar{t}\,\mathcal{P}\mathcal{L}\mathcal{U}(t-\bar{t})\mathcal{Q}\mathcal{L}\mathcal{P}\hat{\rho}(\bar{t}). \tag{B2}$$

Using Eq. (22) it is possible to derive the related equations of motion for the state populations.

Next we note the important properties $\mathcal{P}\mathcal{L}_0=\mathcal{L}_0\mathcal{P}=0$ and $\mathcal{P}\mathcal{L}_V\mathcal{P}=0$. Both relations are simply verified using the definition of the projector and taking into account that H_0 and the dissipative part is diagonal with respect to the electronic states, whereas the transfer coupling has only off-diagonal contributions.

For a further simplification we note $\mathrm{tr}_{\mathrm{vib}}\{\langle\varphi_m|\mathcal{P}\mathcal{L}\hat{O}|\varphi_m\rangle\}=\mathrm{tr}_{\mathrm{vib}}\{\langle\varphi_m|\mathcal{L}_V\hat{O}|\varphi_m\rangle\}$, where $\hat{O}$ has to be identified with respective parts of both terms on the right–hand side of Eq. (B2) [$\hat{O}=\mathcal{P}\hat{\rho}(t)$ as well as $\hat{O}=\mathcal{U}(t-\bar{t})\mathcal{Q}\mathcal{L}\mathcal{P}\hat{\rho}(\bar{t})$]. If we replace $\hat{O}$ by $\mathcal{P}\hat{\rho}$, we easily verify that this term vanishes. The replacement of $\hat{O}$ by $\mathcal{U}(t-\bar{t})\mathcal{Q}\mathcal{L}\mathcal{P}\hat{\rho}(\bar{t})$ leads to the memory kernel of the GME valid for the electronic state populations,

$$\frac{\partial}{\partial t}P_m(t)=\sum_n\int_{-\infty}^{\infty}d\tau\,M_{mn}(\tau)P_n(t-\tau). \tag{B3}$$

Here, we already changed from $\bar{t}$ to $\tau=t-\bar{t}$ and combined the memory kernel with the unit-step function $\Theta(\tau)$. Furthermore, a trace with respect to the complete active system DOF has been introduced to get

$$M_{nm}(t)=-\Theta(t)\mathrm{tr}\{\hat{\Pi}_n\mathcal{L}_V\mathcal{U}(t)\mathcal{Q}\mathcal{L}_V\mathcal{P}\hat{\Pi}_m\}. \tag{B4}$$

Additionally, it was possible to rewrite $\mathcal{Q}\mathcal{L}\hat{r}_n\hat{\Pi}_n$, since we noted the relation $\hat{r}_m\hat{\Pi}_m=\mathcal{P}\hat{\Pi}_m$ and wrote $\mathcal{Q}\mathcal{L}\mathcal{P}\hat{\Pi}_m=\mathcal{Q}\mathcal{L}_V\mathcal{P}\hat{\Pi}_m=\mathcal{L}_V\mathcal{P}\hat{\Pi}_m$.

Equation (B4) will be the starting point for all further considerations. It has been already derived in Refs. 32 and 33 (and discussed more recently in Ref. 31 and 45–47). Here, a generalization is given by taking into account vibrational dissipation via the coupling of the reaction coordinates (active vibrational coordinates) to other thermalized vibrational DOF.

If the memory effects in the GME are of less importance one can change to a standard rate Eq. (13), where the transition rates $k_{m\to n}$ are given by the zero-frequency Fourier transform of M_{nm}, i.e., we get

$$k_{m\to n}=M_{nm}(\omega=0)\equiv-i\mathrm{tr}\{\hat{\Pi}_n\mathcal{L}_V\mathcal{Q}\mathcal{G}(\omega=0)\mathcal{Q}\mathcal{L}_V\mathcal{P}\hat{\Pi}_m\}. \tag{B5}$$

The Green's superoperator $\mathcal{G}(\omega)$ is introduced by noting $\mathcal{Q}\mathcal{L}=\mathcal{L}_0+\mathcal{Q}\mathcal{L}_V$ leading to the following notation for the time-propagation superoperator, Eq. (B1), $\mathcal{U}(t)=\exp\{-i(\mathcal{L}_0+\mathcal{Q}\mathcal{L}_V)t\}$. This expression enables us to formally compute the one-sided Fourier transform of the time-propagation superoperator ($\epsilon\to+0$):

$$\int_0^{\infty}dt\,e^{i\omega t}\mathcal{U}(t)=i(\omega-\mathcal{L}_0-\mathcal{Q}\mathcal{L}_V+i\epsilon)^{-1}\equiv i\mathcal{G}(\omega). \tag{B6}$$

Before introducing a power expansion of M_{nm} we give a formula for the stationary current through the wire based on the GME, Eq. (B3), and used in Sec. VI B for concrete computations.

1. Expression for the stationary current

In the stationary case and at an applied voltage as shown in Fig. 1(b) the stationary current I may be obtained from

$$I \equiv I_L = -e \frac{\partial}{\partial t} \sum_{\mathbf{k}} P_{L\mathbf{k}}(t). \tag{B7}$$

As is well known the time derivative of the electron population has to be replaced by the right-hand side of the respective rate equation. Assuming stationary conditions, the nonlocal expressions in Eq. (B3) reduce to $\Sigma_n M_{mn}(\omega=0) P_n^{(\mathrm{stat})}$, where $P_n^{(\mathrm{stat})}$ denotes the stationary population of level n (the Fermi distribution in the case of the two electrodes). Then it is easy to show that the following current formula becomes valid:

$$I/e = k_{L\to R} - k_{R\to L} + \sum_a \frac{k_{L\to a} k_{a\to R} - k_{R\to a} k_{a\to L}}{k_{a\to L} + k_{a\to R}}. \tag{B8}$$

The concentration on stationary conditions automatically defines the current via the zero-frequency memory kernels, Eq. (B5), i.e., by the ordinary rate expressions $k_{m\to n}$. The first term on the right-hand side of Eq. (B8) is given by direct left-right and right-left transitions which are of fourth order with respect to the electrode-wire coupling. The second term in the above current formula includes all those rates connecting one of the electrodes with one of the wire levels. Those rates, as well as the whole contribution to the current, are of second order with respect to the electrode-wire coupling. The respective expression for the current has been used recently in Ref. 28 to describe charge motion through C_{60} molecules. [However, the approach neglected any formation of coherence described by the first term in Eq. (B8) and considered the vibrational assisted tunneling of the electron through the C_{60} molecule and vibrational relaxation separately.]

2. Perturbational expansion of the memory kernel

The power expansion of M_{nm} with respect to $\mathcal{L}_V$ can be achieved by establishing an equation of motion for $\mathcal{G}(t)$. From Eq. (B6) we can deduce the equation $(\mathcal{G}_0^{-1}(\omega) - \mathcal{Q}\mathcal{L}_V)\mathcal{G}(\omega) = 1$ where a zero-order Greens superoperator has been defined according to $(\omega + i\epsilon - \mathcal{L}_0)\,\mathcal{G}_0(\omega) = 1$. Multiplication by $\mathcal{G}_0(\omega)$ leads to a superoperator version of the ubiquitous Dyson equation $\mathcal{G}(\omega) = \mathcal{G}_0(\omega) + \mathcal{G}_0(\omega)\mathcal{Q}\mathcal{L}_V\mathcal{G}(\omega)$. If rearranged it gives a solution for $\mathcal{G}(\omega)$ in terms of $\mathcal{G}_0(\omega)$ and $\mathcal{Q}\mathcal{L}_V$,

$$\mathcal{G}(\omega) = \sum_{j=0}^{\infty} (\mathcal{G}_0(\omega)\mathcal{Q}\mathcal{L}_V)^j \mathcal{G}_0(\omega). \tag{B9}$$

This expansion is inserted into Eq. (B5) (where we finally can restrict ourselves to even powers of $\mathcal{L}_V$). Let us concentrate on the pure superoperator part first,

$$\mathcal{L}_V\mathcal{Q}\mathcal{G}(\omega)\mathcal{Q}\mathcal{L}_V\mathcal{P} = \sum_{j=0}^{\infty} \mathcal{L}_V\mathcal{Q}(\mathcal{G}_0(\omega)\mathcal{Q}\mathcal{L}_V)^j \mathcal{G}_0(\omega)\mathcal{Q}\mathcal{L}_V\mathcal{P}. \tag{B10}$$

One may use this formula but can also change to a form where the projector $\mathcal{Q}$ is not combined with $\mathcal{L}_V$ but with $\mathcal{G}_0$.

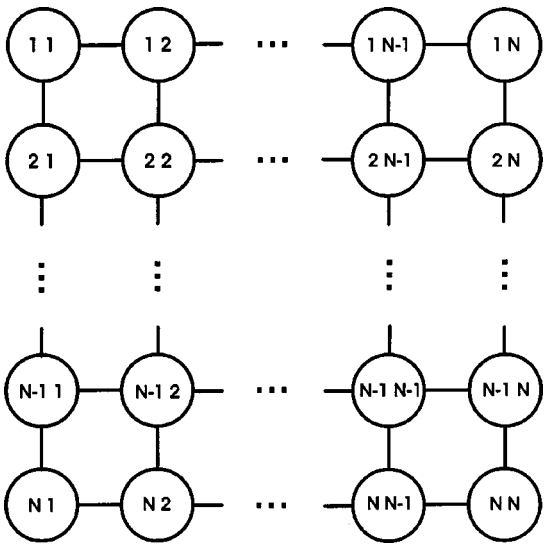

FIG. 11. Liouville space pathways describing different contributions to the memory kernel, Eq. (B13), which refers to the time evolution of the density operator for a transition from state $m=1$ (upper-left corner) to state $n=N$ (lower-right corner). The circle with 11 stands for the elctronic part of the initial value of the density operator $\hat{\rho}(t=0) = \hat{\rho}_{1,1}|\varphi_1\rangle\langle\varphi_1| \equiv r_1\hat{\Pi}_1$. If $\tilde{\mathcal{G}}\mathcal{L}_V$ is applied the action of the respective coupling Hamiltonian may produce density operators with an off-diagonal electronic part, e.g., $\hat{\rho}_{1,2}|\varphi_1\rangle\langle\varphi_2|$ and $\hat{\rho}_{2,1}|\varphi_2\rangle\langle\varphi_1|$. These new density operators are affected by the Green's superoperator $\tilde{\mathcal{G}}$ which corresponds to a dissipative time evolution if translated from the frequency to the time domain. In this manner one proceeds further up to the point where the density operator $\hat{\rho}N,N-1|\varphi N\rangle\langle\varphi N-1|$ or $\hat{\rho}N-1,N|\varphi N-1\rangle\langle\varphi N|$ has been generated [$2(N-1)$ −onefold application of $\tilde{\mathcal{G}}\mathcal{L}_V$.) What remains is the final application of $\mathcal{L}_V$ leading to $\hat{\rho}N,N|\varphi N\rangle\langle\varphi N|$. The resulting rate expression incorporates the $2(N-1)$th power of the coupling operator. It is obvious that the propagation to the final form of the density operator can be achieved in different ways, i.e., by going along different Liouville space pathways.

First, we consider $\mathcal{U}_0(t) = \exp(-i\mathcal{L}_0 t)$ and get $\mathcal{P}\mathcal{U}_0(t) = \mathcal{U}_0(t)\mathcal{P} = \mathcal{P}$, which gives $\mathcal{Q}\mathcal{U}_0(t) = \mathcal{U}_0(t)\mathcal{Q} = \mathcal{U}_0(t) - \mathcal{P} \equiv \mathcal{Q}\mathcal{U}_0(t)\mathcal{Q}$. If changed to the Green's operator $\mathcal{G}_0(\omega)$ it reads (note that the Fourier transform of the unit-step function appears here) $\mathcal{Q}\mathcal{G}_0 = \mathcal{G}_0\mathcal{Q} = \mathcal{Q}\mathcal{G}_0\mathcal{Q} \equiv \tilde{\mathcal{G}}_0$ with

$$\tilde{\mathcal{G}}_0(\omega) = \mathcal{G}_0(\omega) - \frac{1}{\omega + i\epsilon}\mathcal{P}. \tag{B11}$$

Accordingly, the more symmetric version of Eq. (B10) is obtained as

$$\mathcal{L}_V\mathcal{Q}\mathcal{G}(\omega)\mathcal{Q}\mathcal{L}_V\mathcal{P} = \sum_{j=0}^{\infty} \mathcal{L}_V(\tilde{\mathcal{G}}_0(\omega)\mathcal{L}_V)^j \tilde{\mathcal{G}}_0(\omega)\mathcal{L}_V\mathcal{P}. \tag{B12}$$

If combined with the two projection operators $\hat{\Pi}_m$ and $\hat{\Pi}_n$ the resulting frequency-dependent memory kernel reads

$$M_{nm}(\omega) = -i \sum_{j=0}^{\infty} \mathrm{tr}\{\hat{\Pi}_n \mathcal{L}_V(\tilde{\mathcal{G}}_0(\omega)\mathcal{L}_V)^{2j+1}\mathcal{P}\hat{\Pi}_m\}. \tag{B13}$$

This expression serves as a starting point for the consideration of all types of charge-transfer processes through the wire. A graphical representation of Eq. (B13) via so-called Liouville space pathways (see Refs. 33 and 41) together with a detailed explanation are given Fig. 11.

[1] *Molecular Electronic Devices*, edited by F. L. Carter (Dekker, New York, 1982).

[2] *Molecular Electronics: Science and Technology*, edited by A. Aviram (AIP, New York, 1992).

[3] *Molecular Electronics: Properties, Dynamics, and Applications*, edited by G. Mahler, V. May, and M. Schreiber (Dekker, New York, 1996).

[4] *Molecular Electronics: Science and Technolgy*, edited by A. Aviram and M. Ratner (New York Academy of Sciences, New York, 1998).

[5] D. Porath, A. Bezryadin, S. de Vries, and C. Dekker, Nature (London) **403**, 635 (2000).

[6] M. A. Reed, C. Zhou, C. J. Muller, T. P. Burgin, and J. M. Tour, Science **278**, 252 (1997).

[7] J. M. Tour, Acc. Chem. Res. **33**, 791 (2000).

[8] Chem. Phys. **281**, (2002), special issue on *Transport in molecular wires*, edited by P. Hänggi, M. Ratner, and S. Yaliraki.

[9] V. Mujica, M. Kemp, and M. Ratner, J. Chem. Phys. **101**, 6849 (1994); *ibid.* **101**, 6856 (1994).

[10] V. Mujica, M. Kemp, A. Roitberg, and M. Ratner, J. Chem. Phys. **104**, 7296 (1996).

[11] M. Magoga and C. Joachim, Phys. Rev. B **56**, 4722 (1997).

[12] W. Tian, S. Datta, S. Hong, R. Reifenberger, J. I. Henderson, and C. P. Kubiak, J. Chem. Phys. **109**, 2874 (1998).

[13] L. E. Hall, J. R. Reimers, N. S. Hush, and K. Silverbrook, J. Chem. Phys. **112**, 1510 (2000).

[14] V. Mujica, A. Nitzan, Y. Mao, W. Davis, M. Kemp, A. Roitberg, and M. A. Ratner, in Ref. 30.

[15] A. Nitzan, Annu. Rev. Phys. Chem. **52**, 681 (2001).

[16] A. Onipko, Y. Klymenko, and L. Malysheva, Phys. Rev. B **62**, 10 480 (2000).

[17] E. G. Petrov, I. S. Tolokh, A. A. Demidenko, and V. V. Gorbach, Chem. Phys. **193**, 237 (1995).

[18] E. G. Petrov and P. Hänggi, Phys. Rev. Lett. **86**, 2862 (2001).

[19] V. Mujica, A. E. Roitberg, and M. A. Ratner, J. Chem. Phys. **112**, 6834 (2000).

[20] V. May, Physica D **40**, 173 (1989); J. Mol. Electron. **6**, 187 (1990); Phys. Lett. A **161**, 118 (1991).

[21] G. Treboux, J. Phys. Chem. B **104**, 9823 (2000).

[22] M. Olson, Y. Mao, T. Windus, M. Kemp, M. A. Ratner, N. Leon, and V. Mujica, J. Chem. Phys. **102**, 941 (1998).

[23] Z. G. Yu, D. L. Smith, A. Saxena, and A. R. Bishop, Phys. Rev. B **59**, 16 001 (1999).

[24] E. G. Emberly and G. Kirczenow, Phys. Rev. B **61**, 5740 (2000).

[25] M. K. Okuyama and F. G. Shi, Phys. Rev. B **61**, 8224 (2000).

[26] D. Segal, A. Nitzan, W. B. Davis, M. R. Wasielewski, and M. A. Ratner. J. Phys. Chem. B **104**, 3817 (2000).

[27] H. Ness, S. A. Shevlin, and A. J. Fisher, Phys. Rev. B **63**, 125422 (2001).

[28] D. Boese and H. Schoeller, Europhys. Lett. **54**, 668 (2001).

[29] V. May (unpublished).

[30] Adv. Chem. Phys. **106** and **107** (1999), edited by J. Jortner and M. Bixon (series editors I. Prigogine and S. A. Rice).

[31] V. May and O. Kühn, *Charge and Energy Transfer Dynamics in Molecular Systems* (Wiley-VCH, Berlin, 1999).

[32] M. Sparpaglione and S. Mukamel, J. Chem. Phys. **88**, 3263 (1988).

[33] Y. Hu and S. Mukamel, J. Chem. Phys. **91**, 6973 (1989).

[34] K. Blum, *Density Matrix Theory and Applications*, 2nd ed. (Plenum, New York, 1996).

[35] U. Weiss, *Quantum Dissipative Systems* (World Scientific, Singapore, 2000).

[36] S. Datta, *Electronic Transport in Mesoscopic Systems* (Cambridge University Press, Cambridge, England, 1995).

[37] S. A. Gurvitz and Ya. S. Prager, Phys. Rev. B **53**, 15 932 (1996).

[38] S. A. Gurvitz, Phys. Rev. B **57**, 6602 (1998).

[39] M. R. Wegewijs and Yu. V. Nazarov, Phys. Rev. B **60**, 14 318 (1999).

[40] The transmission coefficients also decide in which manner the various wire states are incorporated in the electron transfer reaction. Note that a coupling of different wire levels appears although any interlevel relaxation has been neglected. This is due to a formation of a superposition state of all wire levels if the excess electron is present in the wire. Once such a superposition state is translated into squares of coupling matrix elements two different wire states contribute simultaneously.

[41] S. Mukamel, *Principles of Nonlinear Optical Spectroscopy* (Oxford University, New York, 1995).

[42] The given presentation of the transmission coefficient in the Ω_l-Ω_r plane can be easily related to the transfer rate of donor-bridge-acceptor (DBA) electron transfer. Therefore a certain value of $\hbar\Omega_l$ has to be identified with the donor energy E_D and a value of $\hbar\Omega_r$ with the acceptor energy E_A. Since the frequency integration such as in Eq. (60) vanishes, a direct proportionality of the donor-acceptor rate $k_{D\to A}$ to the transmission coefficient follows. Once the transmission coefficients corresponding to the DBA transfer are drawn in the two-dimensional E_D-E_A representation a multitude of transfer rates $k_{D\to A}$ is given. The difference $E_D - E_A$ gives the so-called driving force of the electron transfer reactions.

[43] $\hbar\Gamma_0$ can be easily estimated if one notes that the density of states can be approximated by the inverse values of 1 or 2 eV, and that for the weak electrode–wire coupling case the respective matrix element V should amount to values in the range of some tens of meV, altogether leading to a $\hbar\Gamma_0$ less than 10 meV. In particular, these values are less than the 40 meV used for the basic vibrational frequency.

[44] O. Linden and V. May, Eur. Phys. J. D **12**, 473 (2000).

[45] S. A. Schofield and P. G. Wolynes, J. Chem. Phys. **100**, 350 (1994).

[46] M. Cho and G.R. Fleming, in Ref. 30, part II, p. 311.

[47] A. A. Golosov and D. R. Reichmann, J. Chem. Phys. **115**, 9848 (2001); *ibid.* **115**, 9862 (2001).